

RESEARCH ARTICLE

Plasmodium falciparum expresses fewer *var* genes at lower levels during asymptomatic dry season infections than clinical malaria cases

Sukai Ceesay^{1,2}, Martin Kampmann^{1,3}, Lasse Votborg-Novél^{1,3}, Helle Smedegaard Hansson⁴, Rasmus Weisel Jensen⁴, Manuela Carrasquilla¹, Hamidou Cisse⁵, Louise Turner⁴, Usama Dabbas¹, Christina Ntalla¹, Silke Bandermann¹, Safiatou Doumbo⁵, Didier Doumtabe⁵, Aissata Ongoiba⁵, Kassoum Kayentao⁵, Boubacar Traore⁵, Peter D. Crompton⁶, Thomas Lavstsen⁴, Silvia Portugal^{1*}

1 Max-Planck-Institute for Infection Biology, Berlin, Germany, **2** Charité – Universitätsmedizin Berlin, Berlin, Germany, **3** Humboldt-Universität zu Berlin, Berlin, Germany, **4** Centre for Translational Medicine and Parasitology, Department of Immunology and Microbiology, University of Copenhagen and Department of Infectious Diseases, Rigshospitalet, Copenhagen, Denmark, **5** Mali International Centre of Excellence in Research, University of Sciences, Techniques and Technologies of Bamako, Bamako, Mali, **6** Laboratory of Immunogenetics, National Institute of Allergy and Infectious Diseases, Division of Intramural Research, National Institutes of Health, Rockville, Maryland, United States of America

☞ These authors contributed equally to this work.

* portugal@mpiib-berlin.mpg.de



OPEN ACCESS

Citation: Ceesay S, Kampmann M, Votborg-Novél L, Hansson HS, Jensen RW, Carrasquilla M, et al. (2025) *Plasmodium falciparum* expresses fewer *var* genes at lower levels during asymptomatic dry season infections than clinical malaria cases. PLoS Pathog 21(6): e1013210. <https://doi.org/10.1371/journal.ppat.1013210>

Editor: Ron Dzikowski, Hebrew University, ISRAEL

Received: January 7, 2025

Accepted: May 12, 2025

Published: June 10, 2025

Peer Review History: PLOS recognizes the benefits of transparency in the peer review process; therefore, we enable the publication of all of the content of peer review and author responses alongside final, published articles. The editorial history of this article is available here: <https://doi.org/10.1371/journal.ppat.1013210>

Copyright: This is an open access article, free of all copyright, and may be freely reproduced, distributed, transmitted, modified, built upon,

Abstract

In seasonal transmission areas, clinical malaria occurs during the wet season when mosquitoes are present, while in the dry season, malaria transmission is interrupted and clinical cases are rare. In Mali, *Plasmodium falciparum* can persist in low parasitaemic asymptomatic individuals through the six-month dry season and shows circulation of more developed parasite stages compared to clinical malaria cases, indicative of reduced cytoadhesion of infected erythrocytes. How prolonged circulation of infected erythrocytes is achieved remains unknown. Here, we explored *var* gene expression in subclinical infections and clinical malaria cases of Malian children, collected during the dry and wet seasons. We sequenced expressed *var* DBL α -tags, used bioinformatic tools to predict their domain composition, binding phenotype and upstream sequence type; and determined their relationship to seasonality and clinical presentation. We found that parasites of asymptomatic infections expressed fewer *var* genes, with a larger proportion of *var* transcripts attributed to one or a few *vars*. In contrast, clinical cases exhibited expression of many *var* genes at lower proportions. We found that parasites of asymptomatic carriers expressed a mixture of CD36- and EPCR-binding PfEMP1, which changed over time. We confirmed that *vars* encoding CD36-binding PfEMP1 dominated in non-severe malaria cases, and found no significant difference in expressed *var* types between dry and wet seasons. Asymptomatic carriers were older, had higher titers of anti-*P. falciparum* antibodies, and broader reactivity to PfEMP1, suggesting that host immunity was the

or otherwise used by anyone for any lawful purpose. The work is made available under the [Creative Commons CC0](https://creativecommons.org/licenses/by/4.0/) public domain dedication.

Data availability statement: Data generated is available in the Edmond repository, is accessible under the following URL: <https://edmond.mpg.de/dataset.xhtml?persistentId=doi:10.17617/3.MUIYC0&faces-redirect=true>

Funding: This work was supported by the European Research Council under the European Union Horizon 2020 Research and Innovation Programme (grant agreement 759534) (SP) and the Lise Meitner Excellence Programme of the Max Planck Society (SP). The Mali cohort study was funded by the Division of Intramural Research, National Institute of Allergy and Infectious Diseases, National Institutes of Health (PDC). The funders had no role in study design, data collection and analysis, decision to publish, or preparation of the manuscript.

Competing interests: The authors have declared that no competing interests exist.

main determinant limiting *var* transcript variation in asymptomatic carriers. However, qRT-PCR analyses also indicated higher total *var* transcript levels in malaria cases compared to asymptomatic carriers, suggesting that in addition to the parasite's switching and the host's immune selection of expressed *var* genes, parasites able to sustain long-term infections may be poised for reduced PfEMP1 expression.

Author summary

In regions like Mali, where malaria is seasonal, *Plasmodium falciparum* can persist in asymptomatic individuals during dry months when mosquito-borne transmission is interrupted. The mechanisms enabling parasite survival in asymptomatic hosts throughout the dry season remain unclear. Here, we investigated expression of the *var* gene family, a key determinant of infected erythrocyte cytoadhesion, throughout the year. Our analyses of DBL α -tag sequences revealed fewer *var* genes expressed in asymptomatic infections, at higher relative proportions; whereas clinical malaria cases exhibited broader *var* gene expression at lower individual proportions. We found no significant seasonal differences in expressed *var* types of *P. falciparum*, and could detect *var* genes switching over time in asymptomatic infections. Asymptomatic carriers were older and had higher anti-*P. falciparum* antibody titers, supporting that host immunity limits *var* transcript diversity. Additionally, we observed significantly lower total *var* transcript levels in asymptomatic infections compared to clinical cases, suggesting that both host immunity and parasite-driven modulation of *var* gene expression contribute to the persistence of *P. falciparum* during the dry season.

Introduction

Plasmodium falciparum remains a major global health problem, leading to over 300 million malaria cases, and 500,000 deaths every year, especially in young African children [1]. To evade host immunity and potentiate persistent infections, parasites possess several multicopy gene families encoding variant surface antigens (VSAs), of which the *P. falciparum* erythrocyte membrane protein 1 (PfEMP1) are particularly important as they mediate the cytoadhesion of the late stage infected red blood cells (iRBC) to specific receptors on the host endothelium [2–4]. Sequestration of iRBCs allows the parasite to avoid the splenic clearance of rigid and deformed iRBCs [5–7], and thus potentiates parasitaemia as well as malaria pathogenesis through blood occlusion and local inflammatory responses to iRBCs [8–15]. Expression on the iRBC surface makes PfEMP1 an immune target and entails switching of expressed variants to evade immunity and prolong infection [16]. Each parasite encodes ~60 *var* genes that are monoallelically expressed [17]. The overall repertoire is extensive [18,19], with new gene variants shuffled through meiotic recombination in the mosquito, and acquisition of mutations and mitotic recombination within the human host [20–26].

Nevertheless, each parasite repertoire is composed of similar *var* gene types, conferring similar repertoires of PfEMP1 phenotypes.

var genes consist of a highly variable Exon 1, encoding the protein's N-terminal extracellular part and the transmembrane domain, and a shorter more conserved Exon 2 encoding the protein's intracellular portion [27]. Most PfEMP1 contain an N-terminal head structure with a Duffy-binding-like (DBL) α domain followed by a Cysteine-rich-interdomain-region (CIDR) domain, followed by 2–6 C-terminal DBL and CIDR domains, a transmembrane domain, and an intracellular acidic terminal segment (ATS) at the C-terminus [27]. Based on chromosomal arrangement and upstream sequence (UPS), *vars* are classified into UPS groups A, B, C, and E [28,29], with each genome typically containing ~10% UPSA, ~75% UPSB and C genes [18] and one UPSE gene also known as *var2csa*. This grouping also reflects the clinical association and the primary receptor binding phenotype of the encoded PfEMP1, determined by the protein's N-terminal domain composition. Thus, *var2csa* PfEMP1 binds placental chondroitin sulphate A and is associated with placental malaria [30,31]. Severe malaria outcomes are linked to PfEMP1 binding endothelial protein C receptor (EPCR) via their CIDR α 1 domains [12,32–34], which are encoded by approximately half of the UPSA *var* genes and a small subset of UPSB *var* genes, which likely arose from UPSB/A recombination events. Most UPSB and UPSC *var* genes encode PfEMP1s that bind CD36 through their CIDR α 2–6 domains, and have been linked to uncomplicated malaria [35–39]. Expression of *var* genes in *P. falciparum* asymptomatic infections is scarcely studied. A few studies suggest a potential association of in asymptomatic infections with UPSC *var* genes [13,40], or report a reduction of UPSA and B but not UPSC in asymptomatic infections vs clinical malaria [41], suggesting a link between *var* gene regulation and asymptomatic infections. Others associate malaria immunity with expression of a restricted *var* repertoire in asymptomatic infection [42], although *var* gene switching appears to continue in longitudinally monitored samples [43]. The ordered nature of PfEMP1 phenotypes and corresponding acquisition of antibodies underlie the quick acquisition of immunity after few severe malaria or pregnancy malaria cases [44,45]. This highlights that host immunity inhibits the growth of parasites expressing certain *vars*, and raises the question of whether, and how, the parasite's *var* repertoire is utilized to facilitate asymptomatic infections bridging wet seasons several months apart.

In areas where malaria is seasonal, transmission is interrupted when mosquito breeding sites are unavailable due to lack of water; and clinical cases are rare [8,46–48]. During a months-long period, asymptomatic infections form the reservoir that restarts transmission in the ensuing wet season [48–50]. These infections exhibit extended circulation of iRBCs compared to those of clinical cases, evidenced by the presence of late ring and trophozoite stages in circulation [8], that is suggestive of reduced cytoadhesion. How the parasite addresses the challenge of persisting silently during periods free of mosquitos, until seasonal rains allow renewed transmission is not known. Here, to interrogate *var* gene expression in subclinical infections and clinical malaria cases of Malians collected during the dry and wet seasons, respectively, we sequenced RT-PCR-amplified *var* cDNA of 82 samples collected from 67 individuals throughout the year.

Results

Expressed DBL α -tag sequencing in a longitudinal cohort in Kalifabougou, Mali

In Kalifabougou, an area of Mali with intense seasonal malaria transmission, we investigated *P. falciparum* parasites from individuals enrolled in a previously described cohort study comprising ~600 individuals from 3 months to 45 years of age [51]. As typical for the region, in 2019, clinical episodes of malaria ($\geq 2,500$ asexual parasites per μ l of blood and axillary temperature ≥ 37.5 °C) were frequent during the wet season (June–December), whereas nearly all individuals remained free of malaria symptoms during the dry season (January–May) (Fig 1A). The prevalence of *P. falciparum* asymptomatic infection was cross-sectionally examined in January, at the beginning (startDry), and in May, at the end (endDry) of the dry season by PCR [52], finding 18% and 10% of positive individuals, respectively. In October (midWet), during the ensuing wet season, 36% of cross-sectionally examined individuals tested positive (Fig 1B), in line with previous descriptions [8,48]. In the cohort, individuals presenting with clinical malaria (MAL) were younger (median 9 years, IQR 3 – 14) than

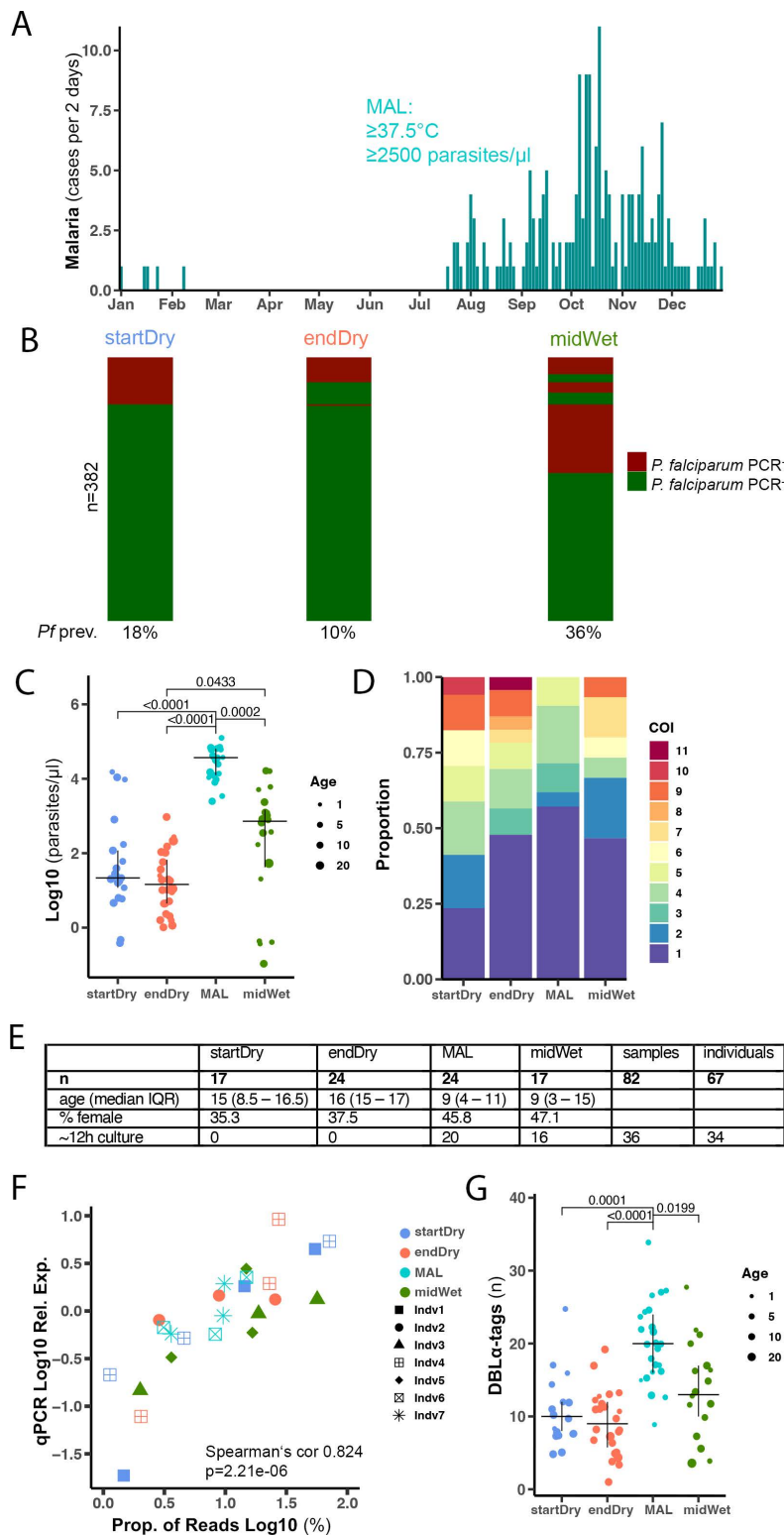


Fig 1. Expressed DBL α -tag sequencing in a longitudinal cohort in Kalifabougou, Mali. (A) Clinical malaria frequency in a cohort of ~600 individuals aged 3 months to 45 years measured every 2 days in 2019, diagnosed by axillary temperature $\geq 37.5^\circ\text{C}$ and $\geq 2,500$ asexual parasites per μl of blood. (B) *P. falciparum* infection prevalence determined by qPCR at the beginning (startDry) and end (endDry) of the dry season, and midway in the wet

season (midWet). Columns are sorted to show the same individual in a single row at all time points. **(C)** Parasitaemia in 104 RDT⁺ samples from startDry (n=30), endDry (n=28), and midWet (n=24) asymptomatic infections, and wet season clinical cases (MAL, n=22) by qPCR of *varATS* relative to a standard curve. **(D)** Proportion of individuals with different complexities of infection (COI) measured as number of *P. falciparum ama1* haplotypes in 79 asymptomatic infections (startDry n=20, endDry n=23, midWet n=15) and 21 clinical malaria cases p-value=0.008 **(E)** Demographics and culture time of samples passing QC in DBL α -tag sequencing **(F)** DBL α -tag read abundance in samples of 7 individuals compared to abundance of the same transcript sequences measured by qPCR relative to a housekeeping gene (Fructose-bisphosphate aldolase, PF3D7_1444800), colour highlights timepoint of collection and shape indicates individual. **(G)** Number of different DBL α -tags observed (0.96 similarity) in clinical cases (n=24), and asymptomatic infections (startDry n=17, endDry n=24, midWet n=17). C & G Data shows median and IQR, dot size indicates participant age. C, D and G Kruskal-Wallis test with Bonferroni multiple comparison correction.

<https://doi.org/10.1371/journal.ppat.1013210.g001>

those with asymptomatic infections in dry (startDry median 14 years, IQR 3 – 16, p=0.0049, and endDry median 15 years, IQR 12 – 16, p<0.0001) or transmission season (midWet median 11 years, IQR 4 – 16, p=0.0067, Dunn's Kruskal-Wallis test). Parasitaemia of 104 samples from 86 individuals, depending on genomic DNA availability, was determined by qPCR of multicopy locus *varATS* [53]. This revealed higher parasitaemia in clinical malaria cases (MAL), intermediate levels in individuals with asymptomatic infections during the wet season (midWet), and lower parasite densities in the dry season samples (startDry and endDry) (Fig 1C), as previously described [54]. Amplicon sequencing of the polymorphic parasite gene *ama1* was used to determine the complexity of infection (COI) of each sample. One to 11 different haplotypes were detected per sample. We observed a higher proportion of monoclonal infections and lower COI in clinical malaria cases (MAL) than in asymptomatic infections (startDry, endDry and midWet) (Fig 1D). The individuals' age correlated negatively to parasitaemia (Spearman's cor -0.39, p=0.000123) (S1A Fig); and positively to COI, when the analysis was done with all samples of all time-points (Spearman's cor. 0.329, p=0.00375) (S1B Fig), but significance was lost when correlations were investigated individually within each timepoint (S1A and B Fig).

To conduct DBL α -tag sequencing, we obtained parasites throughout the year from 118 rapid diagnostic test-positive (RDT⁺) samples of 96 individuals, aged 1–29 years. Samples were collected in the beginning (startDry n=31) and end (endDry n=28) of the dry season from asymptotically infected individuals; and in the ensuing wet season from participants exhibiting their first symptomatic malaria episode of the season (MAL n=29), and from asymptomatic individuals during a cross-sectional timepoint in the middle of the wet season (midWet n=28). Following RNA extraction of all 118 samples, we assessed RNA content by qRT-PCR of two *P. falciparum* housekeeping genes, and selected 93 samples with sufficient expression for DBL α -tag sequencing (startDry n=20, endDry n=28, MAL n=25, midWet n=20), of which 60 samples were prepared in duplicates. DBL α -tags were amplified using a pair of degenerate primers [14]. Samples with <500 sequencing reads across available replicates were excluded, resulting in 82 samples from 67 individuals (startDry n=17, endDry n=24, MAL n=24, midWet n=17, Fig 1E) with 510–107496 reads per sample (median 27467, IQR 14729 – 46464).

Sequencing tags from all 82 samples were pooled and clustered by at least 96% sequence similarity, resulting in 917 unique DBL α -tags (S1 Table). Technical variation between replicates was assessed comparing samples with PCR replicates each comprising >500 reads (n=60). Replicates showed a very strong correlation in reads mapping to specific DBL α -tags (Pearson's cor 0.97, p<2.2e-16, S1C Fig). Of the variants found in the 60 duplicated samples, less than 2% of DBL α -tags were not shared between replicates; hence for all subsequent analyses, replicates, whenever available, were pooled.

The distribution of expressed *var* genes was determined by quantifying the number sequence reads mapping to each of the 917 DBL α -tags. After removal of DBL α -tags with <1% of the total read count in a sample, we obtained a range of 1–35 different DBL α -tags per infection (median 13, IQR 8–18). To validate the DBL α -tag sequencing, we designed three primer-pairs targeting highly and lowly expressed DBL α -tags in eight samples and quantified the *var* transcript levels by qRT-PCR. The sequenced read counts correlated with the qRT-PCR quantification (Fig 1F, Spearman's cor 0.824, p=2.21e-6), confirming that DBL α -tag sequencing could identify *var* gene sequences with good representation of their proportional expression.

Then, we investigated whether DBL α -tag sequences were uniformly distributed throughout the year. We found significantly higher number of different DBL α -tags per sample in clinical malaria cases (MAL) than in dry season asymptomatic infections (startDry, endDry); and a higher number of different DBL α -tags per sample in wet season asymptomatic infections (midWet) compared to the asymptomatic infections from the end of the dry season (endDry) (Fig 1G). First, to rule out a possible sequencing-based systematic bias, we assessed the sequencing reads and found no differences in read counts between timepoints (S1D Fig). Additionally, we examined whether higher numbers of DBL α -tags were driven by more sequencing reads, but found only a weak negative association between read count and number of DBL α -tags per sample (Pearson's cor -0.265, $p=0.016$, S1E Fig). The number of DBL α -tags per sample correlated negatively to the individuals' age (Pearson cor -0.53, $p=3.025e-07$, S1F Fig). However, when timepoints were individually considered, the significant negative correlation between number of DBL α -tags and age was observed only among asymptomatic infections at the start of the dry season (startDry, Spearman's cor 0.57, $p=0.018$, S1F Fig).

To assess whether progression through the 48h IDC led to systematic changes in DBL α -tag expression, we sequenced DBL α -tags on 20 malaria cases (MAL) and 16 asymptomatic infections during the wet season (midWet) following ~12h of in vitro culture to compare with the corresponding ex vivo data of the same samples. We observed a high agreement between ex vivo and ~12h-cultured samples, with a median of 77.5% (IQR 61–84) and 82% (IQR 67–89) of DBL α -tags shared in the asymptomatic and clinical cases, respectively (S2 Fig). DBL α -tags lost during the 12h of culture showed significantly lower expression levels in the corresponding ex vivo sample (median 1.7% of reads IQR 1.3 - 2.7) than those DBL α -tags maintaining detection (median 3.3% of reads IQR 1.8 - 6.5, $p<0.0001$ Kruskal-Wallis test). This suggested that differences between ex vivo and 12h-cultured samples likely resulted from selection of sub-populations of parasites during culture, or differences in detection of low abundance DBL α -tags, and likely not due to variations of developmental stage between dry and wet season samples impacting the DBL α -tag profiles.

Parasites express more *var* genes in malaria cases than in dry season asymptomatic infections

The number of DBL α -tags seen per sample correlated positively with parasitaemia (Spearman's cor 0.46, $p=2.54e-5$, Fig 2A), but no association between the number of DBL α -tags and the sample's COI was observed (Fig 2B). When timepoints were considered separately, we observed a significant positive correlation between number of DBL α -tags and parasitaemia among asymptomatic infections from the start of the dry season (startDry, Spearman's cor 0.57, $p=0.017$, Fig 2A), while other timepoints did not afford statistically significant associations. Among clinical malaria cases, the number of DBL α -tags was positively correlated with COI (Spearman's cor 0.52, $p=0.017$, Fig 2B).

We then investigated proportions of different DBL α -tags identified. This showed that the most abundant DBL α -tag in each clinical malaria case (MAL) comprised a lower proportion of reads compared to the most abundant DBL α -tags in dry season asymptomatic infections (startDry, endDry) (Fig 2C). Accordingly, a higher number of DBL α -tags was required to attain 65% of the DBL α -tag reads in malaria cases compared to asymptomatic infections (S3A Fig). This suggests that the parasite population in clinical malaria cases express many PfEMP1 variants at similar proportions, compared to asymptomatic dry season infections, where a single or few *var* genes dominate expression. Wet season asymptomatic infections showed an intermediate state between the two extremes. Indeed, when we calculated the Simpson Diversity Index of each sample based on the proportions of different DBL α -tags, we found significantly higher values in wet season clinical cases (MAL) compared to dry season asymptomatic infections (startDry, endDry) (S3B Fig).

Our approach allowed tracking of DBL α -tags, as well as *ama1* haplotypes across samples within the population. 131 of 917 DBL α -tags occurred in more than one sample, most of those ($n=102$) were found in two samples; while the most frequent DBL α -tag was found in 20 samples and likely corresponded to *var1*, a conserved, truncated *var* pseudogene (S1 Table). We did not find an association between samples sharing a DBL α -tag and a particular *ama1* haplotype (Chi-squared, $p=0.98$); and we determined that pairs of samples within a timepoint were not more likely to share a DBL α -tag than pairs of samples from different times of the year (Chi-squared, $p=0.73$).

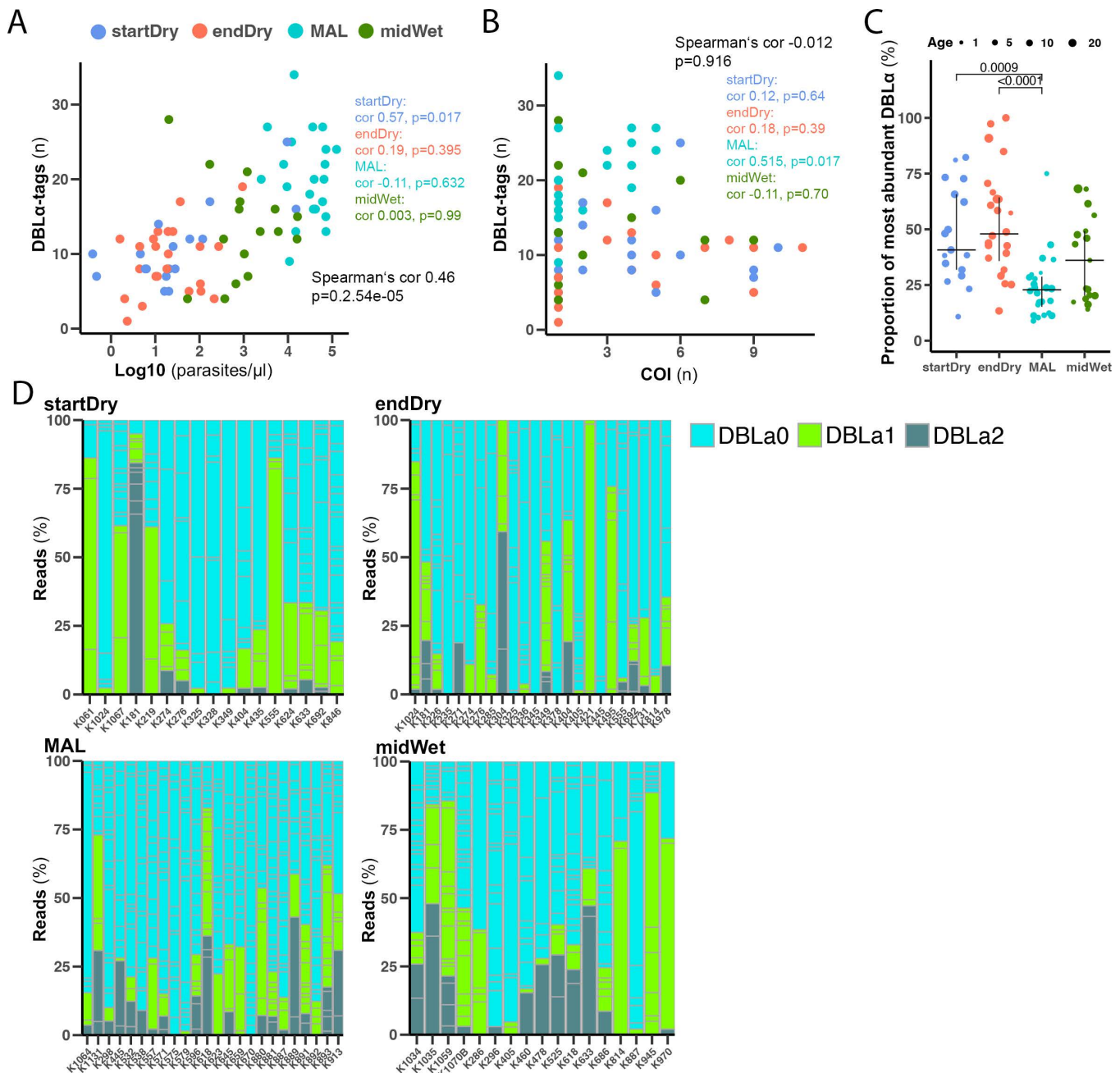


Fig 2. Malaria cases express more *var* genes than dry season asymptomatic infections. (A) Correlation between number of DBLα-tags and parasitaemia measured by *var*ATS-qPCR. (B) Correlation between the number of DBLα tags and COI measured by *ama1*-amplicon sequencing. (C) Proportion of most abundant DBLα-tag at the start (startDry n=17) and end (endDry n=24) of the dry season, in clinical cases (MAL n=24), and midway in the wet season (midWet n=17). Median and IQR are shown, dot size shows participant age, Kruskal-Wallis test with Bonferroni multiple comparison correction. (D) Individual distribution of DBLα-type annotated by best Blast hit in a reference *var* database [56]. Each column represents a person, column sub-divisions show individual DBLα-tags.

<https://doi.org/10.1371/journal.ppat.1013210.g002>

Next, we used a database of *var* genes [18] to annotate our DBL α -tag sequences to DBL α types 0, 1 and 2 [27] by BLAST comparison, based on their best DBL α hit in the database. We found that DBL α 0 was the most represented DBL α type at all timepoints, followed by DBL α 1 and DBL α 2 types (Figs 2D, and S3C), which is in line with the three type's proportion in *P. falciparum* genome [27]. Comparing the reads counts to the different DBL α types, we observed high variability between samples (Fig 2D), but overall, DBL α 0 *var* genes were the most abundant, followed by DBL α 1 and DBL α 2, and no statistically significant difference was seen among the proportion of the three DBL α types across the timepoints (S3D Fig).

For nine of the individuals analysed, paired samples were collected at the beginning (startDry) and end (endDry) of the dry season, when re-infection is unlikely [8,48], prompting us to investigate *var*-gene expression longitudinally. First, we interrogated COI and clonal persistence between the two timepoints using *ama1* sequencing data. Out of eight individuals where *ama1* amplicon sequencing data was obtained at both timepoints, COI was maintained in paired samples over the course of the dry season (startDry 2.5 IQR 2–5; endDry 2 IQR 1–3, Wilcoxon matched-pairs signed-rank test, $p=0.66$). Importantly, in six of the eight individuals (75%), shared clones were detected between the two time points, while random chance of haplotype sharing was ~26%. In four out of the eight samples, *ama1* haplotypes found at the end of the dry season were all already detected at its beginning (S4A Fig). Still, four sample-pairs we also identified potential appearances of new haplotypes at the end the dry season (S4A Fig), which may be attributed to the limit of detection of the method used due to low parasitaemia, and/or cytoadhesion of particular parasite clones at the time of blood draw [55]. DBL α -tag comparisons between samples of the same individual at the beginning and end of the dry season revealed a comparable number of DBL α -tags at the two dry season extremes (startDry 8 IQR 8–11, endDry 12 IQR 10–13, S4B Fig), without significant changes in paired samples (Wilcoxon matched-pairs signed-rank test, $p=0.23$). However, the DBL α -tag expression patterns were highly divergent between paired samples of the two timepoints, indicative of *var* gene switching. In fact, only in one individual (K181, 11.1%), the same DBL α -tag was detected at both time points (S4B Fig), similar to the ~13% chance of finding the same DBL α -tag in two randomly picked samples. In the four paired samples where the *ama1* data revealed that all clones seen at the end of the dry season were present in its beginning, we did not observe any shared DBL α -tags, and no significant difference in the number of DBL α -tags between the two timepoints was observed (S4B Fig, startDry range 8–14, endDry range 10 – 13, Wilcoxon matched-pairs signed-rank test, $p=0.41$), supporting switching of the *var* genes expressed.

Similar *var* gene types and PfEMP1 binding phenotypes predicted in asymptomatic infections and clinical malaria cases

Next, we predicted the domain composition C-terminal to the DBL α domain using Varia [56], and the *var* UPS group using cUPS [57] and the new tool upsAI (Thomas Otto personal communication and <https://github.com/sii-scRNA-Seq/upsAI>). These bioinformatic tools use DBL α -tag sequences and databases of annotated *var* genes to make probabilistic or machine learning predictions about the *var*-encoded domains and UPS region. First, *var* genes were analysed by their mutually exclusive binding phenotypes defined by their predicted N-terminal CIDR domain. *var* transcripts predicted to encode a CIDR α 1 domain were classified as EPCR-binding [32,33], and as CD36-binding if a CIDR α 2–6 domain was predicted [58]. *var* genes predicted to encode CIDR β , γ or δ domains and *var1* were classified as having an unknown binding phenotype ($n=107$, Fig 3A). For 20% ($n=229$) of the DBL α -tags the CIDR domain could not be predicted. This analysis revealed no difference in expression of binding phenotypes between any of the sampling times (Fig 3B). Despite heterogeneity between samples, predicted CD36 binding *var* genes were the most abundant at all timepoints, followed by EPCR-binders (Fig 3A). We then used Varia to predict domains downstream of the first CIDR to identify putative ICAM-1-binding PfEMP1s. These were predicted by the presence of CIDR α 1 and DBL β 1/3, and CIDR α 2–6 and DBL β 5, representing group A and group B ICAM-1-binders, respectively [59]. Putative ICAM-1-binders were very low or absent at all time points, but we detected statistically significant higher expression of group-B ICAM-1-binders in clinical malaria compared to end-dry season infections (S5A Fig). We also quantified expression levels of *vars* encoding DBL δ and DBL γ

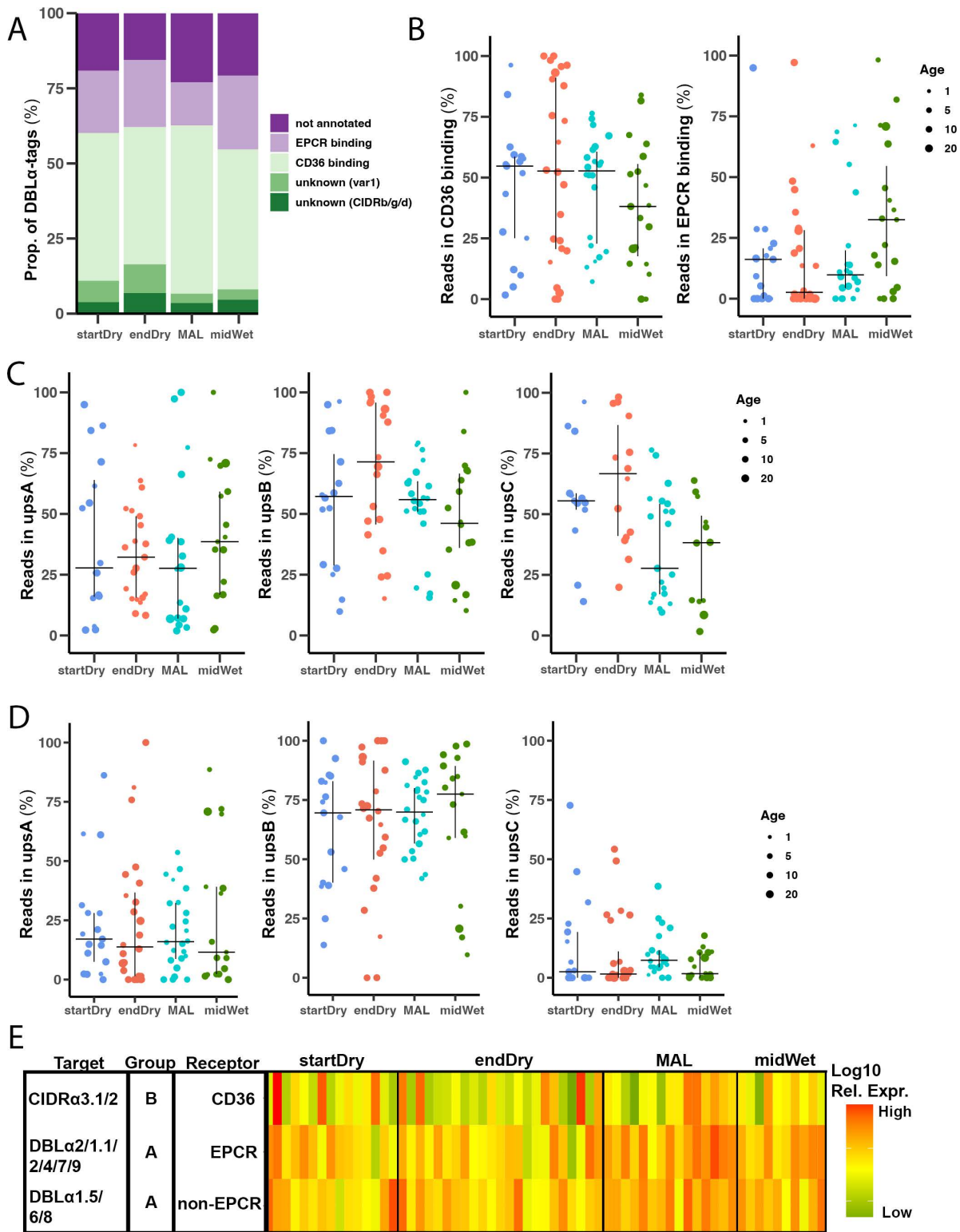


Fig 3. Similar *var* gene types and PfEMP1 binding phenotypes predicted in asymptomatic infections and clinical malaria cases. (A) Proportion of DBL α -tags annotated to PfEMP1 binding type based on domain composition predicted by Varia [56]. Genes were classified as EPCR-binding if the N-terminal CIDR domains was predicted as a non-*var1* CIDR α 1 domain, as CD36-binding if a CIDR α 2 – CIDR α 6 domain was predicted, and as unknown, if prediction corresponded to *var1* or a CIDR β , γ or δ was predicted. (B) Proportion of DBL α -tag reads mapping to *var* genes predicted by

Varia to encode CD36- (left) or EPCR- (right) binding PfEMP1s in the beginning (startDry n = 17) and end (endDry n = 24) of the dry season, during clinical malaria (MAL n = 24), and midway (midWet n = 17) in the wet season. **(C)** Proportion of DBL α -tags mapping to predicted group A (left), B (centre), and C (right) *var* genes using cUPS in the beginning (startDry n = 17) and end (endDry n = 24) of the dry season, in clinical malaria (MAL n = 24), and midway (midWet n = 17) in the wet season using cUSP. **(D)** Proportion of DBL α -tags mapping to predicted group A (left), B (centre), and C (right) *var* genes using cUPS in the beginning (startDry n = 17) and end (endDry n = 24) of the dry season, in clinical malaria (MAL n = 24), and midway (midWet n = 17) in the wet season using upsAI. **(E)** Normalized expression of *var* subtypes in the beginning (startDry n = 15) and end (endDry n = 24) of the dry season, malaria cases (MAL n = 15), and wet season asymptomatic infections (midWet n = 10) by qRT-PCR. DBL α 2/1.1/2/4/7/9 MAL vs endDry (p-value 0.0083. Median and IQR are shown, dot size show participant age; Kruskal-Wallis with Bonferroni correction.

<https://doi.org/10.1371/journal.ppat.1013210.g003>

domains (S5B Fig). As expected, *vars* encoding DBL δ domains found in most *vars* were highly expressed at all timepoints, whereas *vars* predicted to encode DBL γ domains were rare, though a large proportion (45%, n = 504) of DBL α -tags remained unannotated.

We used the cUPS and upsAI tools to assign 68% (n = 772) and 99% (n = 1112), respectively, of the DBL α -tags and to UPSA, B or C (S5C Fig). Both tools predicted similar tags as UPSA *var* genes and gave similar proportions for UPS subtypes but disagreed about assignment of genes between UPSB and UPSC groups. Neither tool resulted in significant differences in abundance between timepoints. In line with genomic proportions [18], UPSB genes were the most expressed at all timepoints, followed by UPSA and UPSC (Fig 3C and D).

To complement the prediction of the domain type composition, we measured expression of a subset of *var* domain types using *var* type-specific primers directly by qRT-PCR in 66 samples (startDry n = 16, endDry n = 24, MAL n = 16, midWet n = 10) for which we also sequenced DBL α -tags. We quantified levels of loci encoding CIDR α 3.1/2 domains as a proxy for CD36-binding *vars*, DBL α 2/1.1/2/4/7/9 for group A EPCR-binding *vars*, and DBL α 1.5/6/8 for group A non-EPCR binding *var*-genes. We observed large variability between samples and mostly non-statistically significant differences in expression level of individual *var* gene types between samples collected in the dry season (startDry and endDry) or during clinical malaria cases in the wet season (MAL) (Figs 3E and S5D), in agreement with the DBL α -tag observations. The only significant difference observed was a higher expression level of group A EPCR-binding *vars* in clinical malaria cases compared to infections at the end of the dry season (S5D Fig). Comparing qRT-PCR measurements and Varia domain predictions in the same samples, we found a significant correlation between relative expression by qRT-PCR and the percentage of reads matching same domain type in DBL α -tag sequencing (CD36-binder: Spearman's cor 0.492, p = 0.000182; EPCR-binder: Spearman's cor 0.323, p = 0.0183; non-EPCR-binder: Spearman's cor 0.441, p = 0.00096, S5E Fig). We also quantified *var2csa* expression by qRT-PCR and detected increased transcript levels in samples of clinical malaria cases in the wet season (MAL n = 15) compared to asymptomatic timepoints of the dry (startDry n = 4, endDry n = 11) and the wet season (midWet n = 10). However, the high *var2csa* level in ex vivo malaria cases was not observed after 12h of in vitro culture of the sample (MAL 12h) (S5F Fig), suggesting that it may be driven by differences in parasite staging [60].

Asymptomatic parasites have lower total *var* transcript levels than clinical malaria parasites

We then investigated the overall *var* transcript level per parasite in clinical malaria cases compared to asymptomatic infections using qRT-PCR primers targeting the acidic terminal segment (*varATS*) [61] in 66 samples collected along the year (startDry n = 17, endDry n = 16, MAL n = 19, midWet n = 14). This showed a significantly higher level of *varATS* transcripts in clinical malaria cases (MAL) compared to asymptomatic infections from the end of the dry season (endDry) and mid of the wet season (midWet), and also compared to all asymptomatic samples combined (Fig 4A). Additionally, we quantified expression of *ruf6*, a non-coding RNA known to regulate transcription of the *var* gene family [62], and observed similar trends to those seen for *varATS* quantification, albeit without statistical significance between any of the individual groups; and with borderline significant differences between *ruf6* in clinical malaria cases (MAL) versus all asymptomatic samples combined (Fig 4B). A strong correlation between *ruf6* expression and the expression of *varATS* was detected (Spearman's cor 0.37, p = 0.0073, Fig 4C). Expression of *varATS* and *ruf6* did not significantly correlate with the number of DBL α -tags

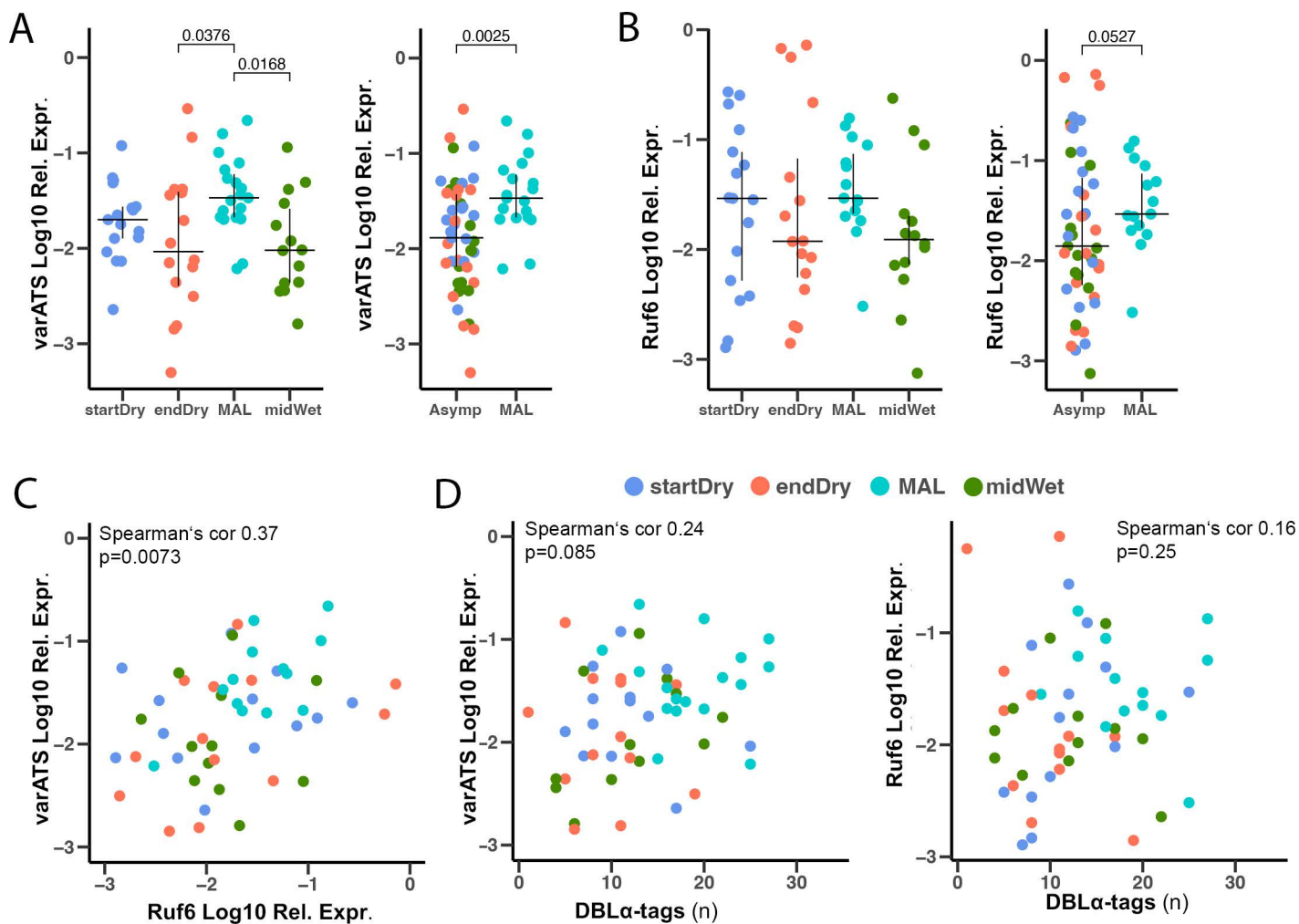


Fig 4. Asymptomatic parasites show lower *var* transcript levels than clinical cases. (A) *varATS* relative expression in asymptomatic infections (startDry n = 17, endDry n = 16, midWet n = 14) and malaria cases (MAL n = 19), measured by qRT-PCR. Samples are divided by time point (left) and clinical status (right). (B) Relative expression of ncRNA *ruf6* in asymptomatic infections (startDry n = 17, endDry n = 16, midWet n = 14) and malaria cases (MAL n = 19) measured by qRT-PCR. Samples are divided by time point (left) and clinical status (right). Median and IQR are shown, Kruskal-Wallis test with Bonferroni correction. (C) Correlation of *varATS* and *ruf6* expression. (D) Correlation of number of DBLα-tags expressed and relative expression of *varATS* (left) and *ruf6* (right).

<https://doi.org/10.1371/journal.ppat.1013210.g004>

found (Spearman's cor *varATS* 0.24, $p=0.085$, *ruf6* 0.16, $p=0.25$, Fig 4D), suggesting that the difference in number of DBLα-tags between samples collected at different times of the year was not explained by differences in total *var* gene expression per iRBC.

Antibody recognition of iRBCs correlates negatively with the number of expressed DBLα-tags

We hypothesized that the more restricted diversity of expressed *var* genes in asymptomatic carriers, compared to clinical cases, was linked to broader and more developed acquired immunity in the older study participants with asymptomatic infections. While we could not quantify antibody responses to the specific PfEMP1 encoded in individual infections, we used three methods to assess humoral immunity to *P. falciparum* antigens. We measured antibodies to AMA1 (a known

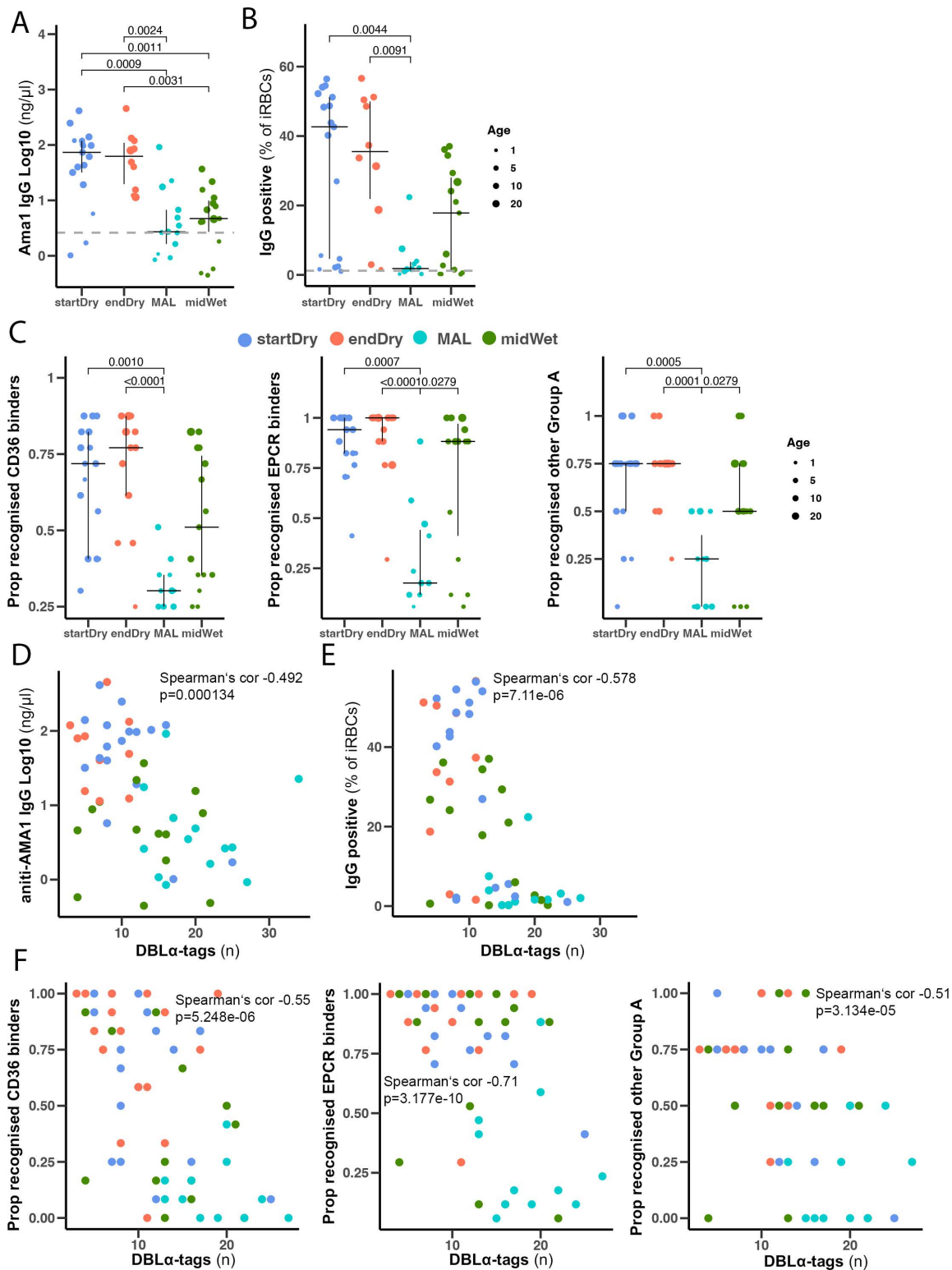


Fig 5. Antibody recognition of iRBC VSAs correlates negatively with the number of expressed DBL α -tags. (A) Plasma anti-AMA1 antibody levels in 54 samples (startDry n=17, endDry n=10, midWet n=15, MAL n=12) measured by ELISA. (B) Surface recognition of PfFCR3 iRBCs by plasma of 54 samples (startDry n=17, endDry n=10, midWet n=15, MAL n=12) measured by flow cytometry. Gray dashed line represents average signal from

naïve plasmas (n=2) (C) Proportion of individuals with antibodies specific to PfEMP1 domains from asymptomatic individuals collected at start (n=17), end of the dry season (n=16), clinical malaria cases (n=11) and mid wet season asymptomatic infections (n=15). Recognition defined as MFI greater than the level in 6 malaria-naïve controls + 2sd in Luminex. Kruskal-Wallis test with Bonferroni multiple comparison correction. (D, E) Correlation of plasma antibody levels measured by AMA1 ELISA (D) and Surface recognition assay (E) with number of DBL α -tag in the same sample. (F) Correlation of proportion of domains recognised and number of DBL α -tags in the same samples.

<https://doi.org/10.1371/journal.ppat.1013210.g005>

marker of cumulative malaria exposure [63]) by ELISA, antibodies to VSAs on PfFCR3 iRBCs predominantly expressing the CD36 and ICAM1-binding IT4VAR16 PfEMP1 variant through a flow cytometry-based surface recognition assay (SRA, gating strategy in S6A Fig), and antibodies to 35 PfEMP1 CIDR domains representing CD36 (n=12) and EPCR (n=17) binding CIDR domains and n=6 other CIDR of group A PfEMP1, through a multiplex bead array [64]. Plasma from asymptomatic dry and wet season samples (startDry n=17, endDry n=10, midWet n=17), and from clinical malaria cases in the wet season (MAL n=10) revealed anti-AMA1 antibodies in most individuals, with significantly higher titers in those maintaining asymptomatic infections during the dry season compared to individuals with clinical malaria or asymptomatic infections in the wet season (Fig 5A). Consistent with the hypothesis that dry season asymptomatic carriers have an increased ability to restrict PfEMP1s, we detected higher surface recognition of VSAs (Fig 5B), and a broader recognition of CD36-, EPCR- and other group A PfEMP1-binders (Fig 5C) in plasma of the dry season asymptomatic infections than in those of clinical malaria cases. Titres of anti-AMA1 antibodies, levels of iRBC surface recognition, and the breadth of the anti-PfEMP1 immune response were highly correlated to each other (S6B, C Fig) and associated with age (S6D Fig). Plasma AMA1 antibody titers, iRBC surface recognition, and broader recognition of PfEMP1 domains of any binding phenotype correlated negatively with the number of DBL α -tags detected in its sample (AMA1: Spearman's cor -0.492, p=0.0001; SRA: Spearman's cor -0.592, p=2.41e-6, CD36 binders: Spearman's cor -0.55 p=5.248e-06, EPCR binders: Spearman's cor -0.71 p=3.177e-10, other group A Spearman's cor -0.51 p=3.134e-05) (Fig 5D-F).

Single-cell RNAseq data supports restricted expression of *var* genes in dry season asymptomatic infections

Finally, we used single-cell SMART-Seq to characterize *var* transcripts and domain architecture obtained from RNA libraries of single FACS-sorted iRBCs of one clinical malaria case (MAL) and one end of the dry season asymptomatic infection (endDry) collected in 2020. Contrasting to DBL α -tag sequencing, SMART-Seq generates reads across the whole *var* gene [65], and hence allowed detecting domains downstream of DBL α without bioinformatic predictions. Both samples were processed ex vivo, and parasites from the clinical malaria case was additionally examined following ~16h of in vitro culture (MAL16h). A total of 115 single FACS-sorted iRBCs (endDry n=54, MAL n=31, MAL16h n=31) were sequenced, and the reads obtained were mapped to a combined *P. falciparum* and human reference. After quality filtering, 111 iRBCs with >100 *P. falciparum* genes and >1000 *P. falciparum* reads, remained for further analyses (endDry n=51, MAL n=29, MAL 16h n=31). First, we assessed whole transcript nucleotide variation across all variant and invariant sites in *P. falciparum* genome using GATK4 [66] to determine the pairwise nucleotide similarity between iRBCs. By hierarchical clustering, iRBCs of the clinical malaria case, independent of culturing, clustered with each other and apart from iRBCs from the end of dry season infection, indicative of one clone in the clinical malaria case and another in the end of the dry season asymptomatic infection (Fig 6A). Parasites were staged by comparison to a single-cell atlas [67], reproducing previously described circulation of older stages in dry-season asymptomatic infections [8]. We then mapped the 111 quality-filtered iRBC transcriptomes to the annotated *var* database of 200,000 *vars* and one million *var* domains [18] used by the Varia and cUPS tools, as limited sequencing coverage precluded *de-novo* assembly of the full *var* genes. Cells were defined as *var*-expressing when more than three reads mapped to the *var* reference and coverage of domains other than the ATS were detected, resulting in 48 and 41 *var*-expressing iRBCs in the dry season and in clinical malaria samples, respectively. We further clustered cells based on *var* domain expression and found 7 clusters of iRBCs expressing similar *var* domains in the end of the dry season iRBCs (Fig 6B) and 22 in the clinical malaria case (Fig 6C), which likely correspond

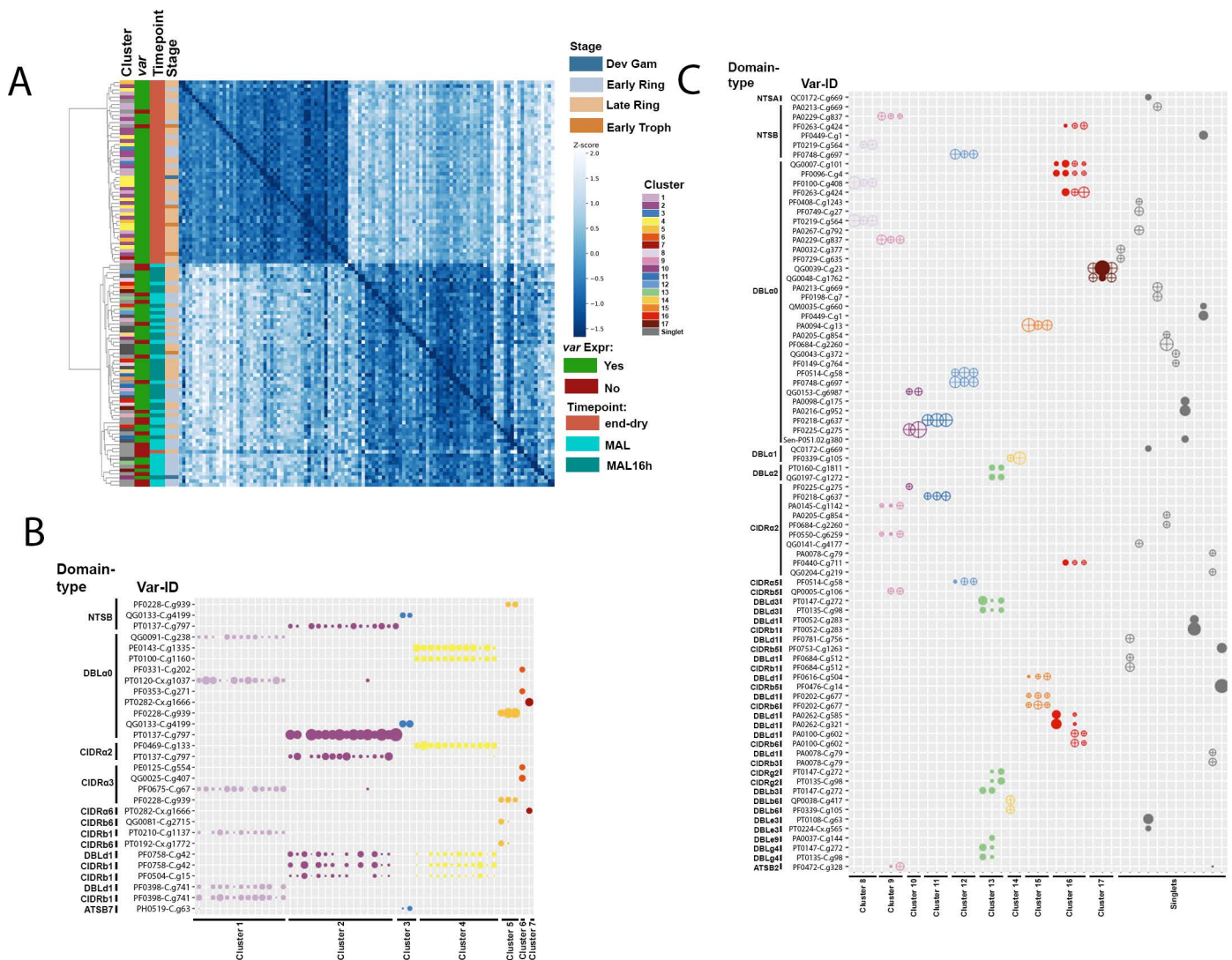


Fig 6. Single Cell RNAseq data supports restricted expression of var genes in dry season asymptomatic infections. (A) Heatmap and hierarchical clustering of z-score values of whole transcriptome nucleotide similarities between single iRBCs of one dry season sample (end-dry, n=51) and one malaria case (MAL, n=29), that additionally was in vitro cultured for ~16h (MAL16h, n=31). Bars next to the heatmap indicate predicted stage, collection timepoint, var expression status and var cluster for each cell. **(B)** Summary of var domain coverage in var-expressing cells of var domains with >1000 normalized reads in at least one cell within the dry season sample (n=48). **(C)** Summary of var domain coverage in var-expressing cells of var domains with >1000 normalized reads in at least one cell of the malaria case sample (n=41). Cells with similar var domain coverage are clustered, cells sequenced ex vivo and after 16h of culture are indicated by circles and crosses, respectively.

<https://doi.org/10.1371/journal.ppat.1013210.g006>

to groups of cells, each expressing a shared var gene. This highlighted a higher number of var domain clusters in the clinical malaria case (5.4 per 10 iRBCs), compared to a lower number of var domain clusters per 10 iRBCs in the end of the dry season sample (1.5 per 10 iRBCs). Similarly, 50% of iRBCs covered a minimum of 2 different var domain clusters in the dry season sample, while they covered at least 7 different var domains in the clinical malaria case, indicating a higher diversity of var gene expression in clinical malaria compared to end of the dry season, as was found by DBLα-tag sequencing (Figs 1 and 2).

For most var domain clusters, we detected DBLα, CIDRα and further downstream domains, though in most clusters at least some domains of a full var gene were missing (S7A-C Fig). In several clusters, we observed mapping to multiple var

domains of the same domain type, which could appear inconsistent with monoallelic expression. We observed 11 of these instances in clusters of the end-dry season sample, and 24 instances in the clinical malaria case's clusters. In *var* cluster 1 of the end-dry season sample, we identified reads of one iRBC mapping to two distinct DBL α 0 sequences, however, the coverage of these two domains did not overlap, suggesting that the sequenced DBL α domain was a combination of separate DBL α sequences found in the database (S7A Fig). More frequently, however, there was ample overlap in the covered regions of similar domain types, indicating multiple highly similar *var* domains in the database, indicating that the specific *var* genes circulating in the samples are not present in the database used for *var* gene mapping, hence our reads mapped to multiple *var* domains of the same domain type within highly similar reference sequences. Indeed, in seven out of ten instances in the end of the dry season clusters (S7A and B Fig), and in all instances in the clinical malaria case' clusters (S7C Fig), pairwise sequence comparison by BLAST revealed high sequence similarity of the covered regions within each instance (median: 99.85%, IQR 98.67-100.00 for the end of the dry season, and median: 99.61%, IQR 96.32-100.00 for the clinical malaria case). In three further instances of mapping to different domains of the same domain type in the end of dry season sample, coverage of one domain type variant was found in the majority of cells in the respective cluster, including a single cell which exclusively also showed lower coverage of another domain type variant. This other domain type variant was also found covered in multiple cells of another cluster with high coverage, suggesting minor cross-contamination between few cells (S7A Fig). All DBL α domains identified in the dry season sample were DBL α 0, while in the malaria case all three types of DBL α were seen, with a minority of DBL α 1 and 2, and the majority of DBL α 0s (Tables S2 and S3). We found CIDR α 2.3/5/8, 3.1/2 and 6 at the end of the dry season, while in the clinical malaria case CIDR α 2.1/2/3/4/9, 3.4, 4, and 5 domains was found (Tables S2 and S3).

Discussion

Studies of *var* expression in clinical cases have linked genes encoding EPCR-binding PfEMP1 to severe malaria, and those encoding CD36-binding PfEMP1 to uncomplicated clinical malaria [40,41,68–70]. However, if and how specific *var* gene and PfEMP1 subsets play a role in the persistence of infection in asymptomatic hosts remains poorly understood. Ruybal-Pesántez and colleagues sequenced DBL α domains of over 1000 parasite genomes of asymptomatic individuals in Ghana, identifying more than 40000 DBL α sequences without reaching coverage saturation of the full *var* gene population, and reported high DBL α diversity in both the wet and the dry seasons [71], suggesting that seasonal selection at the genomic level was unlikely, but expression patterns were not investigated. In this study, we examined expression of *P. falciparum* *var* genes through sequencing of expressed DBL α -tags in 82 samples of 67 Malian children. We identified 917 different DBL α -tags (*var* genes) and validated the relative and absolute transcript levels using primers specific to individual DBL α -tags and the shared *var* exon2 region (*var*ATS qRT-PCR). Overall, parasites from asymptomatic individuals expressed fewer DBL α -tags (Fig 1), showed higher dominance of the most expressed *var* gene (Fig 2) - without preference for a specific *var* UPS type or PfEMP1 binding phenotype (Fig 3) - and had lower total *var* transcripts compared to clinical malaria cases (Fig 4).

Detection of a higher number of different *var* transcripts in clinical malaria cases and its correlation with parasitaemia, was unlikely due to PCR bias [72], as this was minimized by ensuring consistent housekeeping gene expression and gel electrophoresis validation, leading to similar read depths (S1D Fig), strong congruency between replicates (S1C Fig), with findings supported by both qRT-PCR (Figs 1F, and S5E) and SMART-Seq single-cell sequencing (Fig 6).

Few studies have analysed the expressed *var* diversity in asymptomatic individuals. Mugasa and colleagues examined full-length *var* mRNA isolated by magnetic beads tagged with a *var*ATS probe, followed by cloning into vectors and sequencing to compare expression between severe malaria and asymptomatic infections of infants [73]. The authors found no difference in the number of distinct DBL α sequences per isolate between the clinical groups. With the same approach, Falk and colleagues investigated *var* expression in severe, uncomplicated, and asymptomatic children from Papua New Guinea. Also they reported a similar number of DBL α sequences between the three conditions [40]. This

method of amplification, cloning, transfection and sequencing may introduce bias, as the number of unique sequences to be discovered depends on the number of clones sequenced, which is limited and variable between samples, especially since saturating coverage within individuals was not met. The method used in the present study more robustly avoids sampling bias, as the number of potential novel sequences is only limited by sequencing depth and presented no correlation between number of DBL α -tags and sequencing read counts.

In addition to the studies by Mugasa et al. [73] and Falk et al. [40], which reported mixed *var* gene types with a predominance of *vars* encoding CD36-binding group B and C genes, only a few studies have attempted to define the *var* and PfEMP1 types expressed in asymptomatic carriers. Kaestli et al. [13] investigated *var* expression in asymptomatic and clinical malaria in Papua New Guinea using qRT-PCR assay targeting *var* UPS and reported increased UPSC levels in asymptomatic compared to clinical cases. The capture method used to enrich *var* transcripts precluded direct normalization of their expression data, and they instead used genomic DNA of cultured lab strains to calculate *var* copy numbers, which may have introduced bias. In Mkumbaye et al., a lower level of transcripts encoding EPCR-binding PfEMP1 was found in asymptomatic Tanzanian children by qRT-PCR targeting these genes [74]. These studies could not quantify the number of expressed *vars* or the total *var* expression level. The combined DBL α -tag sequencing and *var* type prediction approach used in the present study allowed a higher resolution and more accurate annotation of the expressed *var* genes. However, our approach has limitations as it relies on semi-quantitative PCR amplification using degenerate primers and annotated *var* genes [18] from genomes of the Pf3K and MalariaGEN projects [75]. Nevertheless, we could annotate the majority of amplified tags and found no significant difference in *var* UPS type expression between clinical and asymptomatic infections. Although UPSC *var* genes were the most frequently observed in end of the dry season asymptomatic infections and lowest in clinical malaria by cUPS, these were not statistically significant and not corroborated by upsAI (Fig 3D). Similarly, we observed transcripts representing all PfEMP1 phenotypes, albeit with a dominance of genes encoding CD36-binding PfEMP1 in both asymptomatic and clinical cases. These profiles resemble those previously observed in uncomplicated malaria, and indicate that persistent, asymptomatic infections are not linked to separate *var* gene subset or PfEMP1 phenotype, but is likely associated with the immune status of the individual. Indeed, the present asymptomatic carriers were significantly older and had higher levels of antibodies to both merozoite and VSA antigens, including PfEMP1, than individuals with clinical infections (Fig 5). Warimwe and colleagues have shown in Kenyan children more homogeneous *var* expression in asymptomatic infection associated with a broader host antibody response of slightly older children [42].

IgG targeting and inhibiting PfEMP1 contributes to malaria immunity [76]; and controlled [58] and natural infections [77] of less immune individuals have been linked to expression of a higher number of *var* genes, which is restricted in individuals with higher immunity. Protection from severe malaria is rapidly acquired after a few episodes in areas of high transmission [45], likely due to development of cross-reactive antibodies recognizing PfEMP1-variants associated with severe disease [78]. Thus, acquisition of PfEMP1 antibodies recognising PfEMP1 is ordered, with earlier responses to pathogenic EPCR binding PfEMP1 variants [79,80]. Longer periods of multiple infections seem required to accumulate antibodies recognizing PfEMP1 associated with uncomplicated malaria, finally resulting in mostly avirulent infections in clinically-immune adolescents and adults [51,81,82]. The *var* variants expressed in asymptomatic individuals may represent gaps in the immune coverage of those hosts. However, since we observed all types of *var* genes—including those frequently recognized by exposed individuals—expressed in both clinical and asymptomatic infections, it is plausible that parasites persisting asymptotically over extended periods survive not only by randomly switching to antigenically distinct variants [83], but also by reducing the overall PfEMP1 presentation and cytoadhesion efficiency, rather than relying on specific PfEMP1 types. In support of this notion, we found indications of reduced overall *var* expression in asymptomatic vs clinical malaria cases reported by *var*ATS qPCR primers targeting the semi-conserved and shared *var* exon 2 (Fig 4). Decreased overall *var* expression is also supported by lower the *ruf6* transcripts detected in asymptomatic infections compared to clinical malaria cases (Fig 4). This is in line with findings by Guillochon and colleagues, who assembled de novo *var* gene

expression from RNA-seq of cerebral versus uncomplicated malaria cases and reported lower overall *var* gene expression in uncomplicated cases [84]. Also, a trend of reduced expression of the top *var* gene in asymptomatic end of dry season infections compared to clinical malaria cases described in [8]. Nevertheless, the *var*ATS primers coverage across the *var* family is only ~40%, leaving the possibility of a skewed and not reduced *var* expression. The single cell approach used to validate expression of *var* genes of dry and wet season infections (Fig 6) was also not ideal to corroborate the overall expression level of *var* due to the very small number of cells available and low coverage of *var* genes.

Reduction of adhesin expression and endothelial cell binding capacity in *P. falciparum* has been documented in a splenectomized patient [85], similarly *var* expression can be lost in vitro [86] just as surface expression of PfEMP1 was recently shown to vary independent of *var* transcript level [87].

We also observed higher levels of *var2csa* transcripts in clinical malaria cases compared to dry season asymptomatic infections (S5F Fig). This *var2csa* expression appeared to be transient as it was lost after a short time of in vitro culture. The difference in *var2csa* expression may be driven by differences in parasite stage between clinical and asymptomatic infections, as *var2csa* has also been shown in vitro to peak earlier in its expression than other *var* genes [60]. In vitro, *var2csa* expression depends on the intracellular levels of S-adenosylmethionine (SAM) [88], and its expression has been suggested to play a central role in *var* gene switching [89]; requiring further investigations in natural infections. If, and to what extent, parasites released from the liver include both high and low PfEMP1 expressors, or if such phenotypic variation can arise in blood-stage progeny, remains unclear. Additionally, it is uncertain how low cytoadhesive parasites would survive in individuals with a functioning spleen.

In conclusion, we found that *P. falciparum* parasites from asymptomatic individuals exhibited *var* expression profiles with fewer, more dominant variants compared to clinical infections, likely influenced by host immunity. However, the lower overall *var* transcript abundance and presence of all *var* gene types in asymptomatic carriers suggest that these parasites may represent a subset with particularly efficient switching or reduced cytoadhesion due to lower PfEMP1 presentation.

Materials and methods

Ethics statement

The study was approved by the Ethics Committee of Heidelberg University Hospital; the Faculty of Medicine, Pharmacy and Odontostomatology at the University of Bamako; and the National Institute of Allergy and Infectious Diseases of the National Institutes of Health Institutional Review Board, and is registered at ClinicalTrials.gov (identifier NCT01322581). All study participants or their parents/guardians gave written informed consent to acquisition of samples and clinical data.

Study site and sample collection

Samples and clinical data were obtained in 2019 from a longitudinal cohort study of ~600 individuals aged 3 months to 45 years in Kalifabougou, Mali, as described elsewhere [48,51]. Clinical malaria cases were defined as *Plasmodium* infection with parasitaemia >2500 parasites/ μ l blood and an axillary temperature >37.5°C and no other apparent cause of fever and were treated according to national guidelines with a 3-day course of artemether and lumefantrine. Study exclusion criteria were haemoglobin <7 g/dl, axillary temperature \geq 37.5 °C at enrolment and acute systemic illness or use of antimalarial or immunosuppressive medications in the 30 days preceding enrolment.

Samples used in this study were collected at scheduled cross-sectional timepoints in January, May and October 2019, and in July 2020 as well as during passive surveillance of clinical malaria episodes in 2019 and 2020. At cross-sectional visits and from study participants presenting their first clinical malaria episode during the transmission season 2019, dried blood spots on filter paper (Protein Saver 903, Whatman), thick blood smears and venous blood (4 ml from study participants 4 years or younger, 8 ml from older study participants) were collected. Venous blood was drawn by venipuncture, collected in sodium citrate-containing cell preparation tubes (Vacutainer CPT Tubes, BD) and separated into plasma and

RBC pellets through centrifugation. Subsequently samples were frozen in liquid nitrogen and transported to Heidelberg/Berlin for further analysis.

Detection of clinical malaria and subclinical *P. falciparum* infection

At sample collection timepoints during cross-sectional visits, venous blood samples were tested for subclinical *P. falciparum* infection by rapid diagnostic test (RDT; SD BIOLINE Malaria Ag P.f test of histidine-rich protein II) prior to freezing. Clinical malaria cases were detected by microscopy in Giemsa-stained thick blood smears by light microscopy. *P. falciparum* infection was confirmed retrospectively by nested PCR for the *P. falciparum* 18S rRNA as described elsewhere [52].

P. falciparum short-term culture

Part of RBC pellets of RDT+ asymptomatic samples at the October 2019 cross-sectional timepoint and clinical malaria cases during the transmission season 2019 were cultured prior to freezing at 2% haematocrit in RPMI 1640 (Gibco) complete medium (with L-glutamine and HEPES), 7.4% sodium bicarbonate (Gibco), 100 μ M hypoxanthine (C.C.Pro) and 25 mg/ml gentamycin (Gibco) added with 0.25% Albumax II (Gibco) for 12 h at 37°C in a candle jar as previously described [90]. After 12 h of short-term culture, pellets were collected, frozen in liquid nitrogen and shipped to Heidelberg/Berlin.

Parasitaemia measurement by varATS qPCR

DNA was extracted from frozen RBC pellets using the QIAGEN DNeasy Blood & tissue kit according to manufacturer specifications. qPCR for the varATS locus was performed as previously described [61], using the TaqMan Multiplex Master Mix (Applied biosystems). Quantification was performed based on a standard curve prepared by serial dilution of *in vitro* cultured ring stage *P. falciparum* parasites of a Malian parasite isolate in RBC. Concentrations below 0.1 parasites/ μ l, the lower limit of the standard curve's dynamic range, were considered below the limit of detection.

ama1 amplicon sequencing

DNA was extracted from frozen RBC pellets using the QIAGEN DNeasy Blood & tissue kit. *ama1* amplicon sequencing was performed as previously described [54]. Clusters present in both PCR replicates of a sample and a total read count >500 were included in the analysis.

RNA extraction and cDNA synthesis

RNA was extracted using the phenol-chloroform method performed over 2 days. Frozen RBC pellets were quickly thawed at room temperature and 750 μ l Trizol LS reagent (ambion) added to up to 250 μ l RBCs pellet. The RBC pellet with Trizol mixture was thoroughly mixed by vortexing and the resulting emulsion which was immediately spun at 12,000g for 15 min at 4 °C. The resulting separated top aqueous layer only (without the inter- and organic phase) was transferred into a tube already containing 500 μ l Isopropanol and 3 μ l GlycoBlue and stored overnight at -20 °C. On day 2, the RNA pellet was separated by spinning tubes for 60 min at 12,000g and at 4 °C. This is followed by washing twice in cold ethanol and complete drying of the ethanol from the tube. RNA pellet was resuspended in 20 μ l RNase-free water. Genomic DNA was removed with Amplification grade DNase 1 (invitrogen) according to manufacturer's instructions. To check for effective removal of genomic DNA, 1 μ l of RNA was ran in a qPCR with primers for two *P. falciparum* genes, P61 (fructose-bisphosphate aldolase, PF3D7_1444800) and P90 (serine-tRNA ligase, PF3D7_0717700) using previously designed primers [30,60]. Reactions were set up with Power SYBR Green Master (Applied biosystems), primers were used at a final primer concentration of 1 μ M. Cycling conditions were 10 min 95°C, followed by 30 cycles of 30 sec at 95°C, 40 sec and 50°C, 50 sec at 65°C, and a final elongation of 40 sec at 68°C, followed by a melt curve. qPCRs were run on a

QTower3 (Analytic Jena). cDNA was synthesized with the Superscript IV vilo cDNA Reverse Transcription Kit (invitrogen) using 1 µg of template RNA according to manufacturer specifications.

DBLα-tag sequencing

First, *P. falciparum* transcript abundance in cDNA samples was quantified by qPCR for P61 and P90 housekeeping genes as described above with 2 µl of cDNA as input volume and 40 cycles. Amplification using P61 primers provided higher yield of nucleic acid (lower Ct value) as compared to P90 for the same sample. Therefore, Ct values of P90 primer reactions were used to exclude samples deemed to have too little material for sequencing. Samples with Ct-values >30 for the P90 housekeeping gene were excluded and for samples with Cts between 21–29 subsequent steps were performed in duplicates. As for the samples with Cts of 12 -14.8, the cDNA was diluted 1:100 and for those with Cts > 12 they were diluted 1:1000 prior to subsequent steps. Pre-amplification of DBLα-tag sequencing was performed with the varF_dg2 and Brlong primers. Per reaction, 1 µl of cDNA was mixed with KAPA HiFi fidelity buffer (Roche, 1x final concentration), dNTPs (Roche, final concentration each 0.3 µM), the abovementioned primers (final concentration each 2 µM), at KAPA HiFi Hot-start polymerase (Roche) and run with the following cycling conditions (Table 1).

2 µl of PCR product were run on an agarose gel to inspect product size and primer dimer noise. The expected amplicon size was 350 – 500bp, samples without a visible band at the expected size were excluded. After amplification DBLα-tag sequencing samples were pooled and sequenced on an Illumina MiSeq with 2 × 300 paired-end cycle protocol. Only samples with >500 reads across replicates after quality filtering were included in subsequent analysis (Table 2).

DBLα-tag sequencing bioinformatics

Primer sequences were removed, and adapter and quality trimming performed using trim-galore (<https://github.com/Felix-Krueger/TrimGalore?tab=readme-ov-file>, v. 0.6.10). Processing and filtering of DBLα-tag sequencing followed the steps of the DBLαCleaner pipeline (<https://github.com/UniMelb-Day-Lab/DBLαCleaner/>) [91]. Briefly, paired-end reads were

Table 1. PCR cycling conditions.

Step	Temp (°C)	Duration	Cycles
Hot start	95	2 min	1
Denaturation	98	20 sec	5X
Annealing *	54	30sec (0.5 °C/sec) ramp	
Elongation	68	1 min 15sec (1°C/sec) ramp	
Denaturation	98	20 sec	
Annealing	54	30 sec	30X
Elongation	68	1 min 15sec (1°C/sec) ramp	
Final elongation	72	2 min	
			1

* For the first 5 cycles cooling from denaturation temperature was performed to 65°C at max ramp (3°C/sec), then cooled to 54 °C with 0.5 °C/sec ramp. All other steps ramp 3 °C/sec.

<https://doi.org/10.1371/journal.ppat.1013210.t001>

Table 2. Starting samples and filtering steps.

	startDry	endDry	MAL	midWet	samples	individuals
n	35	29	26	28	118	95
P61/P90 Ct < 30	20	28	25	20	93	75
Visible gel band	18	25	24	17	84	70
>500 reads	17	24	24	17	82	67

<https://doi.org/10.1371/journal.ppat.1013210.t002>

merged using PEAR (v. 0.9.6; -v 10 -n 200) [92]. Merged reads from all samples were concatenated, filtered (--fastq_filter --fastq_maxee 1.0), and overlapping reads collapsed excluding sequences with < 2 reads support (--derep_prefix --minuniquesize 2), and chimeric reads removed (--uchime_denovo) using vsearch v2.15.2 [93]. Remaining sequences were clustered with a 96% nucleotide identity threshold to obtain representative sequence clusters (--cluster-fast -id 0.96). DBL α -tag clusters are referred to as DBL α -tags throughout the manuscript. Non-DBL α -clusters were identified with hmmsearch (HMMER3.3.2, hmmer.org) and excluded, the hmmfile was taken from (<https://github.com/UniMelb-Day-Lab/DBLaCleaner/>). Filtered reads in individual samples were mapped back to remaining DBL α -clusters using vsearch (--usearch_global -id 0.96) to quantify cluster abundance by sample. DBL α -tag sequence clusters were annotated with Varia [56] in GEM mode with default parameters.

Simpson index for a sample was calculated as $1 - \sum (\text{proportion of reads in cluster})^2$. DBL α -tag sequences were translated into amino acids and annotated with cUPS [57] and upsAI (Thomas Otto personal communication and <https://github.com/sii-scRNA-Seq/upsAI>) in tag mode using default parameters. 0.95 probability cutoff was used to assign clusters to upsA, upsB or upsC groups based on the cUPS prediction.

qRT-PCR validation of specific DBL α -tag sequences primer sequences design

For a subset of samples primers specific for individual DBL α -tag-sequences were designed using NCBI primer BLAST [94] by providing the sequence cluster of interest as PCR template. In the primer pair specificity parameters, under database, the option “custom (use your own sequence accession, assembly accession, etc)” was selected and the DBL α -tag sequences of the corresponding sample provided as a fasta file. *Plasmodium* (Laverania) *falciparum* (taxid:5833) was selected under organism name for exclusion. All other parameter values remained as default. The same process was carried out for the highest, one medium, and one low abundance sequence cluster per sample. Even though the default number of designed primers is 10, the first 4 primers were tested in the qRT-PCR validation.

qRT-PCR validation of specific DBL α -tag sequences

For each sequence cluster, 4 different forward and reverse primers were evaluated. All qRT-PCR were performed in 20 μ l reaction volume, primer concentrations of 1 μ M. Each cluster was quantified relative to P90 and P61 housekeeping genes. For each DBL α -tag sequence cluster, a cDNA master-mix for the total number of reactions was prepared containing Power SYBR-green Master Mix 2X, the total required volume of cDNA and nuclease-free water to make up the volume to 18 μ l. The required cDNA volume used was based on the previous P90 housekeeping gene qRT-PCR performed prior to the DBL α -tag sequencing. Samples which had P90 Cts of <15, 1.125 μ l cDNA was added per reaction, those with Cts of 15–19 had 1.25 μ l per reaction and finally the rest of the samples had previous Cts of 22–26 for which 2 μ l of cDNA was added to each reaction. PCR cycling conditions were 10 min at 95 $^{\circ}$ C, followed by 40 cycles of 30 sec at 95 $^{\circ}$ C, 40 sec at 50 $^{\circ}$ C, and 50 sec at 65 $^{\circ}$ C, with final elongation of 40 sec at 68 $^{\circ}$ C followed by a melt curve. All qPCRs were run on a QTower3.

For each DBL α - tag cluster, primer pairs which amplified in reactions with only one melting peak were considered to calculate an average gene Ct relative to their average of Ct P90 and P61 genes.

var domain type qPCR

var-domain type qPCR was performed as described in [14]. Primers for the different domain types were pre-mixed as described in Table 3, to a final total primer concentration of 20 μ M for forward and reverse primers. Primers sequences are found in the Key Resources Table. PCR cycling conditions were 15 min at 95 $^{\circ}$ C, followed by 40 cycles of 30 sec at 95 $^{\circ}$ C, 40 sec at 50 $^{\circ}$ C, and 50 sec at 65 $^{\circ}$ C, with final elongation of 40 sec at 68 $^{\circ}$ C.

Table 3. Primer mix details for different var domain types.

var- domain type	Primer	FW/ REV	H2O (μl)	primer from 100 μM stock (μl)
DBLα1.5/6/8	DBLα1.5/6/8_fwd 1	forward	60	10
	DBLα1.5/6/8_fwd 2	forward		10
	DBLα1.5/6/8_rev 1	reverse		4
	DBLα1.5/6/8_rev 2	reverse		4
	DBLα1.5/6/8_rev 3	reverse		4
	DBLα1.5/6/8_rev 4	reverse		4
	DBLα1.5/6/8_rev 5	reverse		4
DBLα2/1.1/2/4/7/9	DBLα2/1.1/2/4/7/9_fwd 1	forward	60	10
	DBLα2/1.1/2/4/7/9_fwd 2	forward		10
	DBLα2/1.1/2/4/7/9_rev 1	reverse		10
	DBLα2/1.1/2/4/7/9_rev 2	reverse		10
CIDRα3.1/2	CIDRα3.1/2_fwd 1	forward	60	7
	CIDRα3.1/2_fwd 2	forward		7
	CIDRα3.1/2_fwd 3	forward		7
	CIDRα3.1/2_rev 1	reverse		20
Var2csc	Var2csc_fwd	forward	60	20
	Var2csc_rev	reverse		20

<https://doi.org/10.1371/journal.ppat.1013210.t003>

Total var expression by varATS and RUF6 qPCR

Ruf6 and varATS were quantified relative to the housekeeping gene P61. All three genes were quantified on the same day without re-freezing cDNA. P61 qPCR was performed as described above. varATS qPCR was performed using the protocol outlined in [61], using a total reaction volume of 20 μl and 2 μl of cDNA as input. Ruf6 qPCR was performed in 20 μl reaction volume using Power SYBRgreen Master Mix with 2 μl cDNA and the primers Ruf6 A fwd, Ruf6 A rev, Ruf6 B fwd, Ruf6 B rev at a final concentration of 117 nM each. Cycling conditions for Ruf6 qPCR were 10 min at 95°C followed by 40 cycles of 15 sec at 95°C, 20 sec at 54°C, 7 sec at 56.5°C, 7 sec at 59°C and 20 sec at 62°C followed by a melt curve. All qPCRs were run on a QTower3.

AMA1-ELISA

Plasma antibody levels to Ama1 were measured as previously described [95]. Samples were measured in duplicates; quantification was performed relative to a standard curve comprised of wells coated with 250 – 0.244 ng human IgG (biotechne, human IgG Control). Detection was performed using goat-anti Human IgG coupled with alkaline phosphatase (Invitrogen) and 1-Step PNPP solution (Thermo Scientific). All samples were measured at a 1:100 dilution, if samples were outside the dynamic range of the assay, measurements were repeated at higher dilutions (1:200, 1:500, 1:1000) and the average of all dilutions falling in the assay’s dynamic range used. Four plasmas of malaria naïve German donors were used as negative controls. Readout was performed using a SpectraMax 190 plate reader (Molecular Devices) at 405 nm wavelength.

Surface recognition assay

For surface recognition assay, plasmas were heat inactivated for 30 min at 56°C and pre-depleted with uninfected RBCs. FCR3 parasites were panned using HDMEC cells as previously described [96] and used within a week and mainly

expressing IT4var16. Plasmas were incubated at a 1:10 dilution in PBS with FCR3 parasites at 4% Haematocrit, ~2% parasitaemia overnight. Then, parasites were washed three times in PBS and stained with 1:50 anti-human IgG APC (Biolegend) and 1:2000 SYBR green (Invitrogen) in PBS/2%FCS for 30 min at room temperature. After 3x washes in PBS, samples were read in the FITC and APC channels of a flow cytometer (LSR II, BD). A hyperimmune pool and plasmas from two malaria naïve donors were included as positive and negative controls. Analysis was performed using the FlowJo software.

PfEMP1 domain antibody reactivity

Recognition of PfEMP1 domains by plasma antibodies was measured as described in [64]. Briefly, plasma samples were spun down and incubated at 1:40 dilution with PfEMP1 coupled beads for 30 min, followed by 30 min incubation with 1:3000 human secondary F(ab')₂ Goat Anti-Human IgG (Jackson ImmunoResearch) and fluorescence measurement on a Bio-Plex 2000 system. Recognition of individual PfEMP1 domains was defined as fluorescence intensity greater than the average of 6 German malaria-naïve control plasmas plus two standard deviations.

SMART-Seq single-cell RNA-seq

Glycerolyte-frozen RBC pellets of one persisting dry season sample collected at scheduled cross-sectional timepoint in July 2020 and one clinical malaria case in the 2020 wet season were thawed and stained in 1:2000 SYBR green (Invitrogen), 1:25 APC anti-human CD71, clone OKT9 (Invitrogen), and 1:50 APC anti-human Lineage Cocktail (BioLegend) in PBS for 30 min at 37 °C, followed by 3x washes in PBS. Part of the RBC pellet of the clinical malaria case were *in vitro* cultured at 1–2% haematocrit in RPMI 1640 (Gibco) complete medium (with L-glutamine and HEPES), 7.4% sodium bicarbonate (Gibco), 100 μM hypoxanthine (C.C.Pro) and 25 mg ml⁻¹ gentamycin (Gibco) added with 0.25% Albumax II (Gibco) and 10% heat-inactivated O^{RH+} plasma for ~16h at 37°C in a CO₂ incubator (HeraCell VIOS 250i, ThermoFisher) with a gas mixture of 5% O₂, 5% CO₂ and 90% N₂, before staining.

In a flow cytometer (Aria III, BD), FITC-positive and APC-negative iRBCs were single-cell sorted into 96-well PCR plates with lysis buffer (TakaraBio) and flash-frozen on dry-ice followed by storage at -70 °C until further processing. Sequencing libraries were prepared from the cells using the SMART-Seq Single Cell PLUS kit (TakaraBio) and according to the manufacturer's instructions, with 20–21 cycles of cDNA amplification, and 12–16 cycles of library amplification. Quality and quantity of cDNA and libraries were assessed using the Qubit 4.0 1X dsDNA high sensitivity assay (ThermoFisher) and the Bioanalyzer high sensitivity DNA kit (Agilent). The libraries were sequenced on an Illumina MiSeq with 2 × 300 paired-end cycle protocol using the MiSeq Reagent Kit v3 (600-cycle) (Illumina).

Single-cell transcriptome variant analysis

Raw sequencing reads were trimmed for Illumina adapters using cutadapt [97] (-a AGATCGGAAGAGCACACGTCT-GAACTCCAGTCA -A AGATCGGAAGAGCGTCGTGTAGGGAAAGAGTGT -q 30 --pair-filter = any -m 100) and mapped to *P. falciparum* 3D7 (PlasmoDB v60) [98] and human (USCS hg38) [99] using STAR [100] using the '--quantMode GeneCounts' flag to create a gene count matrix, and the '--outSAMtype BAM SortedByCoordinate' to sort the resulting bam file. Gene annotations were obtained from PlasmoDB (v60) and GENCODE (release 34) [101]. The gene count matrix were used to quality-filter the cells (n = 186), keeping cells with >100 Pf genes and >1.000 Pf reads (n = 111), and to determine the parasite developmental stage using the scmapCell function of scmap [102] and the single cell reference atlas of Dogga et al [103]. The Bam files were filtered for mappings to the *Pf* genome and analysed for nucleic acid variations using GATK (v4) [66] with the following series of commands: AddOrReplaceReadGroups (--RGLP ILLUMINA --RGPU MiSeq --RGSM \$cell_id --RGLB \$sample_id), MarkDuplicates, SplitNCigarReads, BaseRecalibrator (--known-sites 3d7_hb3.vcf --known-sites 7g8_gb4.vcf --known-sites hb3_dd2.vcf) [104], ApplyBQSR, HaplotypeCaller (-stand-call-conf 20 --emit-ref-confidence GVCF). The resulting vcf files were analysed using VarClust [105] with modifications in the script.

In brief, each cell was profiled by all variant and non-variant positions with a homozygous call and coverage of at least 5 reads. The profiles were pairwise compared to generate a distance matrix based on matching variant or non-variant calls relative to the overall overlap of positions ($1 - \text{matches/overlap}$). All pairwise comparisons had >5,000 overlapping positions. The `varclust_heatmap` function was used to generate a heatmap with hierarchical clustering based on the distance matrix.

Single-cell *var* gene expression analysis

Trimmed reads of quality-filtered cells ($n = 111$) were mapped to the `varDB` also used for `Varia` (<https://github.com/Thomas-DOtto/varDB/tree/master/Datasets/Varia>). `FeatureCount` [106] (`-p --primary -M -O -f`) was used to generate a *var* domain count matrix, and the cells were filtered by at least 3 mapped reads ($n = 90$) and coverage of more than just ATS domains ($n = 89$). In R, the count matrix was normalized by relative counts and a scaling factor of 10,000, and the *var* domains were filtered by >100 summed normalized reads across cells in a sample. Then, a distance matrix was generated using binary metrics and used for hierarchical clustering using `ward.D2` method [107]. The cells were split into 8 (dry season sample) or 24 (clinical malaria case) clusters, and clusters with similar coverage of NTS, DBL α and/or CIDR α domains were manually collapsed to a total of 7 and 22 clusters, respectively. The covered regions of similar domains were tested for sequence similarity by `megablast` [108] (<https://blast.ncbi.nlm.nih.gov/Blast.cgi?PROGRAM=blastn>).

Supporting information

S1 Fig. DBL α -tag sequencing in clinical and asymptomatic infections from across the year. (A) Correlation of parasitaemia and participant age in October 2019 in 91 samples from beginning of the dry season (startDry $n = 30$), end of the dry season (endDry $n = 28$) and clinical malaria cases (MAL $n = 24$) and the wet season (midWet $n = 22$). (B) Correlation of complexity of infection (COI) and participant age in 79 (startDry ($n = 20$), endDry ($n = 23$) and midWet ($n = 15$)) asymptomatic infections and clinical malaria cases (MAL $n = 21$). (C) Correlation between DBL α -tag abundance between clusters in 60 samples with duplicates of > 500 reads. (D) Read count in 82 samples (startDry = 17, endDry $n = 24$, MAL $n = 24$, midWet $n = 17$) from the four timepoint after quality filtering. (E) Correlation between read count and number of DBL α -tags in a sample with color indicating timepoint. (F) Correlation between number of DBL α -tag clusters in the same samples and participant age with color indicating timepoint.

(TIF)

S2 Fig. DBL α -tag sequencing in clinical and asymptomatic infections after short term culture. Comparison of DBL α -tags in 16 wet season asymptomatic (midWet) samples (left) and 20 MAL (right) *ex vivo* samples (0h) and the corresponding short-term culture timepoints (12h). Individual clusters are plotted on the y-axis with lines connecting clusters detected at the 0h and 12h timepoint. Dot size indicates proportion of reads in sample mapping to the cluster. DBL α -tags were annotated with DBL α subtype by best BLAST hit in a database of annotated *var* genes.

(TIF)

S3 Fig. DBL α -tag cluster distribution in clinical and asymptomatic infections. (A) Minimum number of DBL α -tags in 65% of reads in 82 samples from clinical malaria cases and asymptomatic infections (startDry = 17, endDry $n = 24$, MAL $n = 24$, midWet $n = 17$). Median and IQR are shown with dot size indicating participant age. Kruskal-Wallis test with Bonferroni multiple comparison correction (B) Simpson diversity index of read distribution in the same 82 samples. Median and IQR are shown with dot size indicating participant age. Kruskal-Wallis test with Bonferroni multiple comparison correction. (C) Proportion of DBL α -tags annotated to DBL α -subtypes. Annotation is based on the best Blast hit in an annotated *var* database (min e-value $1e-02$). Shown is the proportion of clusters detected at each of the timepoints belonging to the three DBL α -subtypes. (D) Proportion of DBL α -tag sequencing reads mapping to DBL α -tag clusters annotated as DBL α 0 (left panel), DBL α 1 (middle panel) or DBL α 2 (right panel) in 82 samples across the four timepoints (startDry = 17, endDry

n=24, MAL n=24, midWet n=17). Annotation as described above, median and IQR are indicated on the plot with dot size showing participant age. Kruskal-Wallis test with Bonferroni multiple comparison correction.

(TIF)

S4 Fig. AMA1 amplicon sequencing and DBL α -tag sequencing in paired samples from Jan and May. (A) AMA1 haplotype sharing between paired samples of 8 study participant at the beginning (startDry) and end of the dry season (endDry) 2019. Each box corresponds to a study participant, participant ID is shown in the gray shaded area. Dots represent a haplotype, identifiers are listed on the y-axis, with dot size indicating cluster abundance as proportion of reads. Clusters present at both timepoints are connected by a line. Two replicates per sample, haplotypes were clustered by 0.989 similarity and had to be present in both replicates. Red boxes indicate samples were all haplotypes present at the end of the dry season are also detected at the season's start. (B) DBL α -tag sharing between paired samples of 9 study participants at start and end of the 2019 dry season, each box corresponds to a study participant with ID shown in the gray shaded area. Dots represent a DBL α -tag, shared tags between timepoints are connected by a line. Color indicates annotation by best BLAST hit (min value 1e-02) in an annotated *var* database, abundance as proportion of reads in the sample is shown as dot size. Samples of study participants are shown in the same position in A and B panels.

(TIF)

S5 Fig. *Var*-gene types across timepoints. (A) Expression of putative ICAM1-binding *var* genes in 82 samples (start-Dry = 17, endDry n=24, MAL n=24, midWet n=17). *var* genes with predicted CIDRa1 plus DBL β 1/3, were assigned to group A and CIDRa2 – 6 plus DBL β 5 domains to group B ICAM-1-binders. (B) Expression level of DBL δ and DBL γ containing *var* genes in the same samples. (C) Sankey plot of comparing annotation of DBL α -tags with cUPS and upsAI. (D) Relative expression of different *var*-gene domain types quantified in 54 samples (startDry n= 15, endDry n=24, MAL n= 15, midWet= 10) by qPCR normalized to a housekeeping gene (Fructose-bisphosphate aldolase, PF3D7_1444800). (E) Correlation of relative expression of different *var*-gene domain types measured by RT-qPCR in 54 samples (start-Dry n= 15, endDry n=24, MAL n= 15, midWet= 10) and proportion of reads in DBL α -tag clusters belonging to *var*-genes with the equivalent domain types based on *Varia* prediction in the same samples. Color indicates timepoint. (F) *var2csa* expression in clinical and asymptomatic infections (startDry n=4, endDry n= 11, MAL n= 15, Oct n= 10) and clinical malaria cases after short time of in vitro culture (MAL 12h, n= 15). B, C, E and G Kruskal-Wallis test with Bonferroni multiple comparison correction.

(TIF)

S6 Fig. DBL α -tag sequencing and immunity. (A) Gating strategy of surface recognition assay (SRA) with FCR3 iRBC incubated with plasma of pooled plasma of Malian individuals and stained with SYBRgreen, first gated on single cells based on forward and side scatter (top two small plots each panel) and then on infected RBC based on SYBRgreen staining in the FITC channel (bottom small plot each panel). Surface recognition was identified by staining with an anti-human IgG APC antibody and detected in the APC channel (big plot each panel). (B) Correlation of humoral immunity measured by SRA (left) and AMA1 ELISA (right) in plasmas from dry and wet season (startDry 19 n= 17, endDry n= 10, midWet n= 17, MAL n= 10) to participant age with color indicating timepoint. (C) Correlation of humoral immunity measured by and AMA1 ELISA (top) and SRA (bottom) in the same plasmas and breadth of recognition of *var* domains measured in Luminex. (D) Correlation between the different measures of humoral immunity and participant age. (E) Correlation of humoral immunity measured by AMA1 ELISA (left) and SRA (right) and parasitaemia.

(TIF)

S7 Fig. Sequence comparison of *var* mapping reads in smart-seq data. (A) Comparison of regions with sequencing coverage by smart-seq of an end-Dry season asymptomatic infection. Cells were clustered by *var* expression into 7 clusters indicated by color, and coverage of individual *var* domains in a reference database shown by cluster. The y-axis

delineates identifiers of the individual domains with mapping reads, the x-axis shows sequencing coverage by region of the respective domains. Number of cells with coverage of a specific domain type is shown next to the sequence identifier. 11 instances of reads mapping to different reference domains of the same domain type in the same cluster were detected, highlighted by brackets on the plot. Overlapping regions with coverage in the same cluster (indicated by arrows) were compared by BLAST, sequence similarity of sequences in percent is shown on the right of the respective sequence. In cluster 1, we observed mapping to different regions of different sequences of the same domain type (indicated by dashed line). In cluster 2 and 4, mapping across the majority of cells was congruent, only a single cell showed a divergent expression pattern. **(B)** Proposed *var* gene domain architecture of clusters obtained by single-cell RNAseq of end-dry season sample. Top panel shows domain composition of *var* genes overall, below reference domains detected by single-cell RNA-seq are listed in the corresponding positions for each cluster. **(C)** Equivalent plot to A describing *var* read mapping in a clinical malaria case.

(TIF)

S1 Table. Expression and annotation of individual DBL α -tags in 82 clinical and asymptomatic infections. DBL α -tag sequences were clustered by 0.96 similarity and expression level in individual samples determined. DBL α -tags were annotated using the Varia [56] and cUPS [57] tools, and by the best BLAST hit in an annotated *var* gene database [18]. COI, measured by *ama1* amplicon sequencing and parasitaemia by *var*ATS qPCR are also shown in the table.

(XLSX)

S2 Table. *var* gene expression in single cells from an asymptomatic infection at the end of the dry season by SMARTSeq. Only cells with more than three *var* mapping reads were included. Expression of *var* domains included in a database of 200,000 *vars* and one million *var* domains [19] in the 48 iRBCs collected at the end of the dry season.

(XLSX)

S3 Table. *var* gene expression in single cells from a clinical malaria case in the wet season by SMARTSeq. Only cells with more than three *var* mapping reads were included. Expression of *var* domains included in a database of 200,000 *vars* and one million *var* domains [19] in the 41 iRBCs collected during a clinical malaria case in the wet season.

(XLSX)

S4 Table. Key resources table.

(DOCX)

Acknowledgments

We thank the residents of Kalifabougou, Mali, for their participation in the study. Recombinant AMA1 protein was kindly provided by Karthik Gunalan and Louis H Miller, NIH. Katrin Lehmann and Mir-Farzin Mashreghi at DRFZ assisted the sequencing of the SMART-seq libraries on the MiSeq. We thank Aaron Pangilinan and Thomas Otto (University of Glasgow) for sharing upsAI tool prior to its publication. We acknowledge the use of PlasmoDB (<https://plasmodb.org>) throughout this study and thank its team for maintaining this valuable resource.

Author contributions

Conceptualization: Sukai Ceesay, Martin Kampmann, Lasse Votborg-Novél, Thomas Lavstsen, Silvia Portugal.

Data curation: Sukai Ceesay, Martin Kampmann, Lasse Votborg-Novél, Helle Smedegaard Hansson, Rasmus Weisel Jensen.

Formal analysis: Sukai Ceesay, Martin Kampmann, Lasse Votborg-Novél, Silvia Portugal.

Funding acquisition: Peter D Crompton, Thomas Lavstsen, Silvia Portugal.

Investigation: Sukai Ceesay, Martin Kampmann, Lasse Votborg-Novél, Helle Smedegaard Hansson, Rasmus Weisel Jensen, Manuela Carrasquilla, Hamidou Cisse, Louise Turner, Usama Dabbas, Christina Ntalla, Silke Bandermann, Aissata Ongoiba, Silvia Portugal.

Methodology: Sukai Ceesay, Martin Kampmann, Lasse Votborg-Novél, Helle Smedegaard Hansson, Rasmus Weisel Jensen, Manuela Carrasquilla, Hamidou Cisse, Louise Turner, Usama Dabbas, Christina Ntalla, Silke Bandermann, Thomas Lavstsen, Silvia Portugal.

Project administration: Boubacar Traore, Peter D Crompton, Silvia Portugal.

Resources: Safiatou Doumbo, Didier Doumtabe, Aissata Ongoiba, Kassoum Kayentao, Boubacar Traore, Peter D Crompton, Silvia Portugal.

Software: Martin Kampmann, Lasse Votborg-Novél.

Supervision: Boubacar Traore, Peter D Crompton, Thomas Lavstsen, Silvia Portugal.

Validation: Martin Kampmann.

Visualization: Sukai Ceesay, Martin Kampmann, Lasse Votborg-Novél.

Writing – original draft: Sukai Ceesay, Martin Kampmann, Lasse Votborg-Novél, Thomas Lavstsen, Silvia Portugal.

Writing – review & editing: Sukai Ceesay, Martin Kampmann, Lasse Votborg-Novél, Helle Smedegaard Hansson, Rasmus Weisel Jensen, Manuela Carrasquilla, Hamidou Cisse, Louise Turner, Usama Dabbas, Christina Ntalla, Silke Bandermann, Safiatou Doumbo, Didier Doumtabe, Aissata Ongoiba, Kassoum Kayentao, Boubacar Traore, Peter D Crompton, Thomas Lavstsen, Silvia Portugal.

References

1. WHO, World malaria report 2023. 2023.
2. Baruch DI, Gormely JA, Ma C, Howard RJ, Pasloske BL. Plasmodium falciparum erythrocyte membrane protein 1 is a parasitized erythrocyte receptor for adherence to CD36, thrombospondin, and intercellular adhesion molecule 1. *Proc Natl Acad Sci U S A*. 1996;93(8):3497–502. <https://doi.org/10.1073/pnas.93.8.3497> PMID: 8622965
3. Smith JD, Chitnis CE, Craig AG, Roberts DJ, Hudson-Taylor DE, Peterson DS, et al. Switches in expression of Plasmodium falciparum var genes correlate with changes in antigenic and cytoadherent phenotypes of infected erythrocytes. *Cell*. 1995;82(1):101–10. [https://doi.org/10.1016/0092-8674\(95\)90056-x](https://doi.org/10.1016/0092-8674(95)90056-x) PMID: 7606775
4. Su XZ, Heatwole VM, Wertheimer SP, Guinet F, Herrfeldt JA, Peterson DS, et al. The large diverse gene family var encodes proteins involved in cytoadherence and antigenic variation of Plasmodium falciparum-infected erythrocytes. *Cell*. 1995;82(1):89–100. [https://doi.org/10.1016/0092-8674\(95\)90055-1](https://doi.org/10.1016/0092-8674(95)90055-1) PMID: 7606788
5. Miller LH. Distribution of mature trophozoites and schizonts of Plasmodium falciparum in the organs of Aotus trivirgatus, the night monkey. *Am J Trop Med Hyg*. 1969;18(6):860–5.
6. Hommel M, David PH, Oligino LD. Surface alterations of erythrocytes in Plasmodium falciparum malaria. Antigenic variation, antigenic diversity, and the role of the spleen. *J Exp Med*. 1983;157(4):1137–48. <https://doi.org/10.1084/jem.157.4.1137> PMID: 6187885
7. Roberts DJ, et al. Rapid switching to multiple antigenic and adhesive phenotypes in malaria. *Nature*. 1992;357(6380):689–92.
8. Andrade CM, et al. Increased circulation time of Plasmodium falciparum underlies persistent asymptomatic infection in the dry season. *Nat Med*. 2020.
9. Thomson-Luque R, Votborg-Novél L, Ndovie W, Andrade CM, Niangaly M, Attipa C, et al. Plasmodium falciparum transcription in different clinical presentations of malaria associates with circulation time of infected erythrocytes. *Nat Commun*. 2021;12(1):4711. <https://doi.org/10.1038/s41467-021-25062-z> PMID: 34330920
10. Jespersen JS, Wang CW, Mkumbaye SI, Minja DT, Petersen B, Turner L, et al. Plasmodium falciparum var genes expressed in children with severe malaria encode CIDRa1 domains. *EMBO Mol Med*. 2016;8(8):839–50. <https://doi.org/10.15252/emmm.201606188> PMID: 27354391
11. Storm J, Craig AG. Pathogenesis of cerebral malaria— inflammation and cytoadherence. *Front Cell Infect Microbiol*. 2014;4:100. <https://doi.org/10.3389/fcimb.2014.00100> PMID: 25120958
12. Turner L, Lavstsen T, Berger SS, Wang CW, Petersen JEV, Avril M, et al. Severe malaria is associated with parasite binding to endothelial protein C receptor. *Nature*. 2013;498(7455):502–5. <https://doi.org/10.1038/nature12216> PMID: 23739325

13. Kaestli M, Cockburn IA, Cortés A, Baea K, Rowe JA, Beck H-P. Virulence of malaria is associated with differential expression of *Plasmodium falciparum* var gene subgroups in a case-control study. *J Infect Dis*. 2006;193(11):1567–74. <https://doi.org/10.1086/503776> PMID: [16652286](https://pubmed.ncbi.nlm.nih.gov/16652286/)
14. Lavstsen T, Turner L, Saguti F, Magistrado P, Rask TS, Jespersen JS, et al. *Plasmodium falciparum* erythrocyte membrane protein 1 domain cassettes 8 and 13 are associated with severe malaria in children. *Proc Natl Acad Sci U S A*. 2012;109(26):E1791–800. <https://doi.org/10.1073/pnas.1120455109> PMID: [22619319](https://pubmed.ncbi.nlm.nih.gov/22619319/)
15. Storm J, Jespersen JS, Seydel KB, Szeszak T, Mbewe M, Chisala NV, et al. Cerebral malaria is associated with differential cytoadherence to brain endothelial cells. *EMBO Mol Med*. 2019;11(2):e9164. <https://doi.org/10.15252/emmm.201809164> PMID: [30610112](https://pubmed.ncbi.nlm.nih.gov/30610112/)
16. Scherf A, Hernandez-Rivas R, Buffet P, Bottius E, Benatar C, Pouvelle B, et al. Antigenic variation in malaria: in situ switching, relaxed and mutually exclusive transcription of var genes during intra-erythrocytic development in *Plasmodium falciparum*. *EMBO J*. 1998;17(18):5418–26. <https://doi.org/10.1093/emboj/17.18.5418> PMID: [9736619](https://pubmed.ncbi.nlm.nih.gov/9736619/)
17. Chen Q, Fernandez V, Sundström A, Schlichtherle M, Datta S, Hagblom P, et al. Developmental selection of var gene expression in *Plasmodium falciparum*. *Nature*. 1998;394(6691):392–5. <https://doi.org/10.1038/28660> PMID: [9690477](https://pubmed.ncbi.nlm.nih.gov/9690477/)
18. Otto TD, Assefa SA, Böhme U, Sanders MJ, Kwiatkowski D, Pf3k consortium, et al. Evolutionary analysis of the most polymorphic gene family in *falciparum* malaria. *Wellcome Open Res*. 2019;4:193. <https://doi.org/10.12688/wellcomeopenres.15590.1> PMID: [32055709](https://pubmed.ncbi.nlm.nih.gov/32055709/)
19. Barry AE, Leliwa-Sytek A, Tavul L, Imrie H, Migot-Nabias F, Brown SM, et al. Population genomics of the immune evasion (var) genes of *Plasmodium falciparum*. *PLoS Pathog*. 2007;3(3):e34. <https://doi.org/10.1371/journal.ppat.0030034> PMID: [17367208](https://pubmed.ncbi.nlm.nih.gov/17367208/)
20. Frank M, Kirkman L, Costantini D, Sanyal S, Lavazec C, Templeton TJ, et al. Frequent recombination events generate diversity within the multi-copy variant antigen gene families of *Plasmodium falciparum*. *Int J Parasitol*. 2008;38(10):1099–109. <https://doi.org/10.1016/j.ijpara.2008.01.010> PMID: [18395207](https://pubmed.ncbi.nlm.nih.gov/18395207/)
21. Freitas-Junior LH, Bottius E, Pirrit LA, Deitsch KW, Scheidig C, Guinet F, et al. Frequent ectopic recombination of virulence factor genes in telomeric chromosome clusters of *P. falciparum*. *Nature*. 2000;407(6807):1018–22. <https://doi.org/10.1038/35039531> PMID: [11069183](https://pubmed.ncbi.nlm.nih.gov/11069183/)
22. Rask TS, et al. *Plasmodium falciparum* erythrocyte membrane protein 1 diversity in seven genomes—divide and conquer. *PLoS Comput Biol*. 2010;6(9).
23. Sander AF, Lavstsen T, Rask TS, Lisby M, Salanti A, Fordyce SL, et al. DNA secondary structures are associated with recombination in major *Plasmodium falciparum* variable surface antigen gene families. *Nucleic Acids Res*. 2014;42(4):2270–81. <https://doi.org/10.1093/nar/gkt1174> PMID: [24253306](https://pubmed.ncbi.nlm.nih.gov/24253306/)
24. Zhang X, Alexander N, Leonardi I, Mason C, Kirkman LA, Deitsch KW. Rapid antigen diversification through mitotic recombination in the human malaria parasite *Plasmodium falciparum*. *PLoS Biol*. 2019;17(5):e3000271. <https://doi.org/10.1371/journal.pbio.3000271> PMID: [31083650](https://pubmed.ncbi.nlm.nih.gov/31083650/)
25. Bopp SER, et al. Mitotic evolution of *Plasmodium falciparum* shows a stable core genome but recombination in antigen families. *PLoS Genetics*. 2013;9(2):e1003293–e1003293.
26. Claessens A, Hamilton WL, Kekre M, Otto TD, Faizullahoy A, Rayner JC, et al. Generation of antigenic diversity in *Plasmodium falciparum* by structured rearrangement of Var genes during mitosis. *PLoS Genet*. 2014;10(12):e1004812. <https://doi.org/10.1371/journal.pgen.1004812> PMID: [25521112](https://pubmed.ncbi.nlm.nih.gov/25521112/)
27. Rask TS, et al. *Plasmodium falciparum* erythrocyte membrane protein 1 diversity in seven genomes – divide and conquer. *PLOS Computational Biology*. 2010;6(9):e1000933.
28. Lavstsen T, Salanti A, Jensen ATR, Arnot DE, Theander TG. Sub-grouping of *Plasmodium falciparum* 3D7 var genes based on sequence analysis of coding and non-coding regions. *Malar J*. 2003;2:27. <https://doi.org/10.1186/1475-2875-2-27> PMID: [14565852](https://pubmed.ncbi.nlm.nih.gov/14565852/)
29. Kraemer SM, Smith JD. Evidence for the importance of genetic structuring to the structural and functional specialization of the *Plasmodium falciparum* var gene family. *Mol Microbiol*. 2003;50(5):1527–38. <https://doi.org/10.1046/j.1365-2958.2003.03814.x> PMID: [14651636](https://pubmed.ncbi.nlm.nih.gov/14651636/)
30. Salanti A, Staaloe T, Lavstsen T, Jensen ATR, Sowa MPK, Arnot DE, et al. Selective upregulation of a single distinctly structured var gene in chondroitin sulphate A-adhering *Plasmodium falciparum* involved in pregnancy-associated malaria. *Mol Microbiol*. 2003;49(1):179–91. <https://doi.org/10.1046/j.1365-2958.2003.03570.x> PMID: [12823820](https://pubmed.ncbi.nlm.nih.gov/12823820/)
31. Salanti A, Dahlbäck M, Turner L, Nielsen MA, Barfod L, Magistrado P, et al. Evidence for the involvement of VAR2CSA in pregnancy-associated malaria. *J Exp Med*. 2004;200(9):1197–203. <https://doi.org/10.1084/jem.20041579> PMID: [15520249](https://pubmed.ncbi.nlm.nih.gov/15520249/)
32. Jespersen JS, Wang CW, Mkumbaye SI, Minja DT, Petersen B, Turner L, et al. *Plasmodium falciparum* var genes expressed in children with severe malaria encode CIDRα1 domains. *EMBO Mol Med*. 2016;8(8):839–50. <https://doi.org/10.15252/emmm.201606188> PMID: [27354391](https://pubmed.ncbi.nlm.nih.gov/27354391/)
33. Mkumbaye SI, et al. The severity of *Plasmodium falciparum* infection is associated with transcript levels of var genes encoding endothelial protein C receptor-binding *P. falciparum* erythrocyte membrane protein 1. *Infection and Immunity*. 2017;85(4).
34. Shabani E, Hanisch B, Opoka RO, Lavstsen T, John CC. *Plasmodium falciparum* EPCR-binding PfEMP1 expression increases with malaria disease severity and is elevated in retinopathy negative cerebral malaria. *BMC Med*. 2017;15(1):183. <https://doi.org/10.1186/s12916-017-0945-y> PMID: [29025399](https://pubmed.ncbi.nlm.nih.gov/29025399/)
35. Cabrera A, Neculai D, Kain KC. CD36 and malaria: friends or foes? A decade of data provides some answers. *Trends Parasitol*. 2014;30(9):436–44. <https://doi.org/10.1016/j.pt.2014.07.006> PMID: [25113859](https://pubmed.ncbi.nlm.nih.gov/25113859/)

36. Ochola LB, Siddondo BR, Ocholla H, Nkya S, Kimani EN, Williams TN, et al. Specific receptor usage in *Plasmodium falciparum* cytoadherence is associated with disease outcome. *PLoS One*. 2011;6(3):e14741. <https://doi.org/10.1371/journal.pone.0014741> PMID: 21390226
37. Hsieh F-L, Turner L, Bolla JR, Robinson CV, Lavstsen T, Higgins MK. The structural basis for CD36 binding by the malaria parasite. *Nat Commun*. 2016;7:12837. <https://doi.org/10.1038/ncomms12837> PMID: 27667267
38. Robinson BA, Welch TL, Smith JD. Widespread functional specialization of *Plasmodium falciparum* erythrocyte membrane protein 1 family members to bind CD36 analysed across a parasite genome. *Mol Microbiol*. 2003;47(5):1265–78. <https://doi.org/10.1046/j.1365-2958.2003.03378.x> PMID: 12603733
39. Bachmann A, et al. CD36-A host receptor necessary for malaria parasites to establish and maintain infection. *Microorganisms*. 2022;10(12).
40. Falk N, et al. Analysis of *Plasmodium falciparum* var genes expressed in children from Papua New Guinea. *J Infect Dis*. 2009;200(3):347–56.
41. Rottmann M, et al. Differential expression of var gene groups is associated with morbidity caused by *Plasmodium falciparum* infection in Tanzanian children. *Infect Immun*. 2006;74(7):3904–11.
42. Warimwe GM, et al. *Plasmodium falciparum* var gene expression homogeneity as a marker of the host-parasite relationship under different levels of naturally acquired immunity to malaria. *PLoS One*. 2013;8(7):e70467.
43. Kaestli M, Cortes A, Lagog M, Ott M, Beck H-P. Longitudinal assessment of *Plasmodium falciparum* var gene transcription in naturally infected asymptomatic children in Papua New Guinea. *J Infect Dis*. 2004;189(10):1942–51. <https://doi.org/10.1086/383250> PMID: 15122533
44. Fried M, Nosten F, Brockman A, Brabin BJ, Duffy PE. Maternal antibodies block malaria. *Nature*. 1998;395(6705):851–2. <https://doi.org/10.1038/27570> PMID: 9804416
45. Gupta S, Snow RW, Donnelly CA, Marsh K, Newbold C. Immunity to non-cerebral severe malaria is acquired after one or two infections. *Nat Med*. 1999;5(3):340–3. <https://doi.org/10.1038/6560> PMID: 10086393
46. Lehmann T, et al. Aestivation of the African malaria mosquito, *Anopheles gambiae* in the Sahel. *The American Journal of Tropical Medicine and Hygiene*. 2010;83(3):601–6.
47. Dao A, Yaro AS, Diallo M, Timbiné S, Huestis DL, Kassogué Y, et al. Signatures of aestivation and migration in Sahelian malaria mosquito populations. *Nature*. 2014;516(7531):387–90. <https://doi.org/10.1038/nature13987> PMID: 25470038
48. Portugal S, et al. Treatment of chronic asymptomatic *Plasmodium falciparum* infection does not increase the risk of clinical malaria upon reinfection. *Clin Infect Dis*. 2017;64(5):645–53.
49. Ouédraogo AL, Gonçalves BP, Gnémé A, Wenger EA, Guelbeogo MW, Ouédraogo A, et al. Dynamics of the human infectious reservoir for malaria determined by mosquito feeding assays and ultrasensitive malaria diagnosis in burkina faso. *J Infect Dis*. 2016;213(1):90–9. <https://doi.org/10.1093/infdis/jiv370> PMID: 26142435
50. Babiker HA, Abdel-Muhsin AM, Ranford-Cartwright LC, Satti G, Walliker D. Characteristics of *Plasmodium falciparum* parasites that survive the lengthy dry season in eastern Sudan where malaria transmission is markedly seasonal. *Am J Trop Med Hyg*. 1998;59(4):582–90. <https://doi.org/10.4269/ajtmh.1998.59.582> PMID: 9790434
51. Tran TM, Li S, Doumbo S, Doumtabe D, Huang C-Y, Dia S, et al. An intensive longitudinal cohort study of Malian children and adults reveals no evidence of acquired immunity to *Plasmodium falciparum* infection. *Clin Infect Dis*. 2013;57(1):40–7. <https://doi.org/10.1093/cid/cit174> PMID: 23487390
52. Snounou G, Viriyakosol S, Zhu XP, Jarra W, Pinheiro L, do Rosario VE, et al. High sensitivity of detection of human malaria parasites by the use of nested polymerase chain reaction. *Mol Biochem Parasitol*. 1993;61(2):315–20. [https://doi.org/10.1016/0166-6851\(93\)90077-b](https://doi.org/10.1016/0166-6851(93)90077-b) PMID: 8264734
53. Hofmann N, Mwingira F, Shekalaghe S, Robinson LJ, Mueller I, Felger I. Ultra-sensitive detection of *Plasmodium falciparum* by amplification of multi-copy subtelomeric targets. *PLoS Med*. 2015;12(3):e1001788. <https://doi.org/10.1371/journal.pmed.1001788> PMID: 25734259
54. Andrade CM, et al. Infection length and host environment influence on *Plasmodium falciparum* dry season reservoir. *EMBO Mol Med*. 2024.
55. Färnert A, Lebbad M, Faraja L, Rooth I. Extensive dynamics of *Plasmodium falciparum* densities, stages and genotyping profiles. *Malar J*. 2008;7:241. <https://doi.org/10.1186/1475-2875-7-241> PMID: 19025582
56. Mackenzie G, Jensen RW, Lavstsen T, Otto TD. *Varia*: a tool for prediction, analysis and visualisation of variable genes. *BMC Bioinformatics*. 2022;23(1):52. <https://doi.org/10.1186/s12859-022-04573-6> PMID: 35073845
57. Tan MH, et al. A paradoxical population structure of var DBLα types in Africa. *bioRxiv*. 2023.
58. Bachmann A, Bruske E, Krumkamp R, Turner L, Wichers JS, Petter M, et al. Controlled human malaria infection with *Plasmodium falciparum* demonstrates impact of naturally acquired immunity on virulence gene expression. *PLoS Pathog*. 2019;15(7):e1007906. <https://doi.org/10.1371/journal.ppat.1007906> PMID: 31295334
59. Joste V, et al. PfEMP1 A-Type ICAM-1-Binding domains are not associated with cerebral malaria in beninese children. *mBio*. 2020;11(6).
60. Dahlbäck M, et al. Changes in var gene mRNA levels during erythrocytic development in two phenotypically distinct *Plasmodium falciparum* parasites. *Malaria Journal*. 2007;6(1):78.
61. Hofmann N, Mwingira F, Shekalaghe S, Robinson LJ, Mueller I, Felger I. Ultra-sensitive detection of *Plasmodium falciparum* by amplification of multi-copy subtelomeric targets. *PLoS Med*. 2015;12(3):e1001788. <https://doi.org/10.1371/journal.pmed.1001788> PMID: 25734259
62. Diffendall GM, et al. Discovery of RUF6 ncRNA-interacting proteins involved in *P. falciparum* immune evasion. *Life Sci Alliance*. 2023;6(1).

63. van den Hoogen LL, Stresman G, Pr sum  J, Romilus I, Mond lus G, Elism  T, et al. Selection of antibody responses associated with plasmodium falciparum infections in the context of malaria elimination. *Front Immunol*. 2020;11:928. <https://doi.org/10.3389/fimmu.2020.00928> PMID: 32499783
64. Obeng-Adjei N, Larremore DB, Turner L, Ongoiba A, Li S, Doumbo S, et al. Longitudinal analysis of naturally acquired PfEMP1 CIDR domain variant antibodies identifies associations with malaria protection. *JCI Insight*. 2020;5(12):e137262. <https://doi.org/10.1172/jci.insight.137262> PMID: 32427581
65. Wang X, et al. Direct comparative analyses of 10X genomics chromium and smart-seq2. *Genomics Proteomics Bioinformatics*. 2021;19(2):253–66.
66. Auwera G v d, O'Connor BD. *Genomics in the cloud: using Docker, GATK, and WDL in Terra*. First edition ed. Sebastopol, CA: O'Reilly Media. 2020.
67. Votborg-Novel L, et al. Seasonal transcriptional profiling of malaria parasites using a new single-cell atlas of a Malian Plasmodium falciparum isolate. *bioRxiv*. 2025:2025.04.14.648697.
68. Kyriacou HM, Stone GN, Challis RJ, Raza A, Lyke KE, Thera MA, et al. Differential var gene transcription in Plasmodium falciparum isolates from patients with cerebral malaria compared to hyperparasitaemia. *Mol Biochem Parasitol*. 2006;150(2):211–8. <https://doi.org/10.1016/j.molbiopara.2006.08.005> PMID: 16996149
69. Warimwe GM, Fegan G, Musyoki JN, Newton CRJC, Opiyo M, Githinji G, et al. Prognostic indicators of life-threatening malaria are associated with distinct parasite variant antigen profiles. *Sci Transl Med*. 2012;4(129):129ra45. <https://doi.org/10.1126/scitranslmed.3003247> PMID: 22496547
70. Jensen AT, et al. Plasmodium falciparum associated with severe childhood malaria preferentially expresses PfEMP1 encoded by group A var genes. *J Exp Med*. 2004;199(9):1179–90.
71. Ruybal-Pes ntez S, Tiedje KE, Pilosof S, Tonkin-Hill G, He Q, Rask TS, et al. Age-specific patterns of DBL  var diversity can explain why residents of high malaria transmission areas remain susceptible to Plasmodium falciparum blood stage infection throughout life. *Int J Parasitol*. 2022;52(11):721–31. <https://doi.org/10.1016/j.ijpara.2021.12.001> PMID: 35093396
72. Lapp Z, Freedman E, Huang K, Markwalter CF, Obala AA, Prudhomme-O'Meara W, et al. Analytic optimization of Plasmodium falciparum marker gene haplotype recovery from amplicon deep sequencing of complex mixtures. *PLOS Glob Public Health*. 2024;4(5):e0002361. <https://doi.org/10.1371/journal.pgph.0002361> PMID: 38814915
73. Mugasa J, et al. Genetic diversity of expressed Plasmodium falciparum var genes from Tanzanian children with severe malaria. *Malaria Journal*. 2012;11(1):230.
74. Mkumbaye SI, et al. The severity of Plasmodium falciparum infection is associated with transcript levels of var genes encoding endothelial protein C receptor-binding P. falciparum erythrocyte membrane protein 1. *Infect Immun*. 2017;85(4).
75. Ahouidi A, Ali M, Almagro-Garcia J, Amambua-Ngwa A, Amaratunga C, et al. An open dataset of Plasmodium falciparum genome variation in 7,000 worldwide samples. *Wellcome Open Res*. 2021;6:42. <https://doi.org/10.12688/wellcomeopenres.16168.2> PMID: 33824913
76. David PH, Hommel M, Miller LH, Udeinya IJ, Oligino LD. Parasite sequestration in Plasmodium falciparum malaria: spleen and antibody modulation of cytoadherence of infected erythrocytes. *Proc Natl Acad Sci U S A*. 1983;80(16):5075–9. <https://doi.org/10.1073/pnas.80.16.5075> PMID: 6348780
77. Wichers JS, et al. Common virulence gene expression in adult first-time infected malaria patients and severe cases. *Elife*. 2021;10.
78. Turner L, Lavstsen T, Mmbando BP, Wang CW, Magistrado PA, Vestergaard LS, et al. IgG antibodies to endothelial protein C receptor-binding cysteine-rich interdomain region domains of Plasmodium falciparum erythrocyte membrane protein 1 are acquired early in life in individuals exposed to malaria. *Infect Immun*. 2015;83(8):3096–103. <https://doi.org/10.1128/IAI.00271-15> PMID: 26015475
79. Cham GK, et al. Hierarchical, domain type-specific acquisition of antibodies to Plasmodium falciparum erythrocyte membrane protein 1 in Tanzanian children. *Infect Immun*. 2010;78(11):4653–9.
80. Obeng-Adjei N, et al. Longitudinal analysis of naturally acquired PfEMP1 CIDR domain variant antibodies identifies associations with malaria protection. *JCI Insight*. 2020.
81. Marsh K, Kinyanjui S. Immune effector mechanisms in malaria. *Parasite Immunol*. 2006;28(1–2):51–60.
82. Weiss GE, Traore B, Kayentao K, Ongoiba A, Doumbo S, Doumbo D, et al. The Plasmodium falciparum-specific human memory B cell compartment expands gradually with repeated malaria infections. *PLoS Pathog*. 2010;6(5):e1000912. <https://doi.org/10.1371/journal.ppat.1000912> PMID: 20502681
83. Recker M, Buckee CO, Serazin A, Kyes S, Pinches R, Christodoulou Z, et al. Antigenic variation in Plasmodium falciparum malaria involves a highly structured switching pattern. *PLoS Pathog*. 2011;7(3):e1001306. <https://doi.org/10.1371/journal.ppat.1001306> PMID: 21408201
84. Guillochon E, et al. Transcriptome analysis of Plasmodium falciparum isolates from Benin reveals specific gene expression associated with cerebral malaria. *The Journal of Infectious Diseases*. 2022;225(12):2187–96.
85. Bachmann A, Esser C, Petter M, Predehl S, von Kalkreuth V, Schmiedel S, et al. Absence of erythrocyte sequestration and lack of multicopy gene family expression in Plasmodium falciparum from a splenectomized malaria patient. *PLoS One*. 2009;4(10):e7459. <https://doi.org/10.1371/journal.pone.0007459> PMID: 19826486
86. Florini F, et al. Transcriptional plasticity of virulence genes provides malaria parasites with greater adaptive capacity for avoiding host immunity. *bioRxiv*. 2024.
87. Cronshagen J, et al. A system for functional studies of the major virulence factor of malaria parasites. *eLife Sciences Publications*; 2024.

88. Schneider VM, Visone JE, Harris CT, Florini F, Hadjimichael E, Zhang X, et al. The human malaria parasite *Plasmodium falciparum* can sense environmental changes and respond by antigenic switching. *Proc Natl Acad Sci U S A*. 2023;120(17):e2302152120. <https://doi.org/10.1073/pnas.2302152120> PMID: 37068249
89. Zhang X, Florini F, Visone JE, Lionardi I, Gross MR, Patel V, et al. A coordinated transcriptional switching network mediates antigenic variation of human malaria parasites. *Elife*. 2022;11:e83840. <https://doi.org/10.7554/eLife.83840> PMID: 36515978
90. Trager W, Jensen JB. Human malaria parasites in continuous culture. *Science*. 1976;193(4254):673–5. <https://doi.org/10.1126/science.781840> PMID: 781840
91. He Q, Pilosof S, Tiedje KE, Ruybal-Pesántez S, Artzy-Randrup Y, Baskerville EB, et al. Networks of genetic similarity reveal non-neutral processes shape strain structure in *Plasmodium falciparum*. *Nat Commun*. 2018;9(1):1817. <https://doi.org/10.1038/s41467-018-04219-3> PMID: 29739937
92. Zhang J, Kobert K, Flouri T, Stamatakis A. PEAR: a fast and accurate Illumina Paired-End reAd mergeR. *Bioinformatics*. 2014;30(5):614–20. <https://doi.org/10.1093/bioinformatics/btt593> PMID: 24142950
93. Rognes T, Flouri T, Nichols B, Quince C, Mahé F. VSEARCH: a versatile open source tool for metagenomics. *PeerJ*. 2016;4:e2584. <https://doi.org/10.7717/peerj.2584> PMID: 27781170
94. Ye J, Coulouris G, Zaretskaya I, Cutcutache I, Rozen S, Madden TL. Primer-BLAST: a tool to design target-specific primers for polymerase chain reaction. *BMC Bioinformatics*. 2012;13:134. <https://doi.org/10.1186/1471-2105-13-134> PMID: 22708584
95. Miura K, Orcutt AC, Muratova OV, Miller LH, Saul A, Long CA. Development and characterization of a standardized ELISA including a reference serum on each plate to detect antibodies induced by experimental malaria vaccines. *Vaccine*. 2008;26(2):193–200. <https://doi.org/10.1016/j.vaccine.2007.10.064> PMID: 18054414
96. Attaher O, Mahamar A, Swihart B, Barry A, Diarra BS, Kanoute MB, et al. Age-dependent increase in antibodies that inhibit *Plasmodium falciparum* adhesion to a subset of endothelial receptors. *Malar J*. 2019;18(1):128. <https://doi.org/10.1186/s12936-019-2764-4> PMID: 30971252
97. Martin M. Cutadapt removes adapter sequences from high-throughput sequencing reads. *Bioinformatics*. 2011;17(1):3.
98. Aurrecochea C, Brestelli J, Brunk BP, Dommer J, Fischer S, Gajria B, et al. PlasmoDB: a functional genomic database for malaria parasites. *Nucleic Acids Res*. 2009;37(Database issue):D539–43. <https://doi.org/10.1093/nar/gkn814> PMID: 18957442
99. Casper J, et al. The UCSC Genome Browser Database: 2018 Update. *Nucleic Acids Res*. 2018;46(D1):D762–9.
100. Dobin A, Davis CA, Schlesinger F, Drenkow J, Zaleski C, Jha S, et al. STAR: ultrafast universal RNA-seq aligner. *Bioinformatics*. 2013;29(1):15–21. <https://doi.org/10.1093/bioinformatics/bts635> PMID: 23104886
101. Harrow J, et al. GENCODE: the reference human genome annotation for The ENCODE Project. *Genome Research*. 2012;22(9):1760–74.
102. Kiselev VY, Yiu A, Hemberg M. scmap: projection of single-cell RNA-seq data across data sets. *Nat Methods*. 2018;15(5):359–62. <https://doi.org/10.1038/nmeth.4644> PMID: 29608555
103. Dogga SK, Rop JC, Cudini J, Farr E, Dara A, Ouologuem D, et al. A single cell atlas of sexual development in *Plasmodium falciparum*. *Science*. 2024;384(6695):eadj4088. <https://doi.org/10.1126/science.adj4088> PMID: 38696552
104. Miles A, Iqbal Z, Vauterin P, Pearson R, Campino S, Theron M, et al. Indels, structural variation, and recombination drive genomic diversity in *Plasmodium falciparum*. *Genome Res*. 2016;26(9):1288–99. <https://doi.org/10.1101/gr.203711.115> PMID: 27531718
105. FASTERUS E, Uhlén M, Al-Khalili Szgyarto C. Single-cell RNA-seq variant analysis for exploration of genetic heterogeneity in cancer. *Sci Rep*. 2019;9(1):9524. <https://doi.org/10.1038/s41598-019-45934-1> PMID: 31267007
106. Liao Y, Smyth GK, Shi W. featureCounts: an efficient general purpose program for assigning sequence reads to genomic features. *Bioinformatics*. 2014;30(7):923–30. <https://doi.org/10.1093/bioinformatics/btt656> PMID: 24227677
107. Murtagh F, Legendre P. Ward's hierarchical agglomerative clustering method: which algorithms implement Ward's criterion?. *Journal of Classification*. 2014;31(3):274–95.
108. Altschul SF, Madden TL, Schäffer AA, Zhang J, Zhang Z, Miller W, et al. Gapped BLAST and PSI-BLAST: a new generation of protein database search programs. *Nucleic Acids Res*. 1997;25(17):3389–402. <https://doi.org/10.1093/nar/25.17.3389> PMID: 9254694